# Spectroscopy of $^{98}$Ru

A. Giannatiempo,[1] A. Nannini,[2] A. Perego,[1,2] and P. Sona[1]
[1]*Dipartimento di Fisica e Astronomia, Università di Firenze, IT-50019 Sesto Fiorentino (Firenze), Italy*
[2]*Istituto Nazionale di Fisica Nucleare, Sezione di Firenze, IT-50019 Sesto Fiorentino (Firenze), Italy*
(Received 29 July 2016; published 29 November 2016)

The $^{98}$Ru nucleus, populated via the $^{97}$Mo($^3$He,$2n$) reaction, has been investigated by means of $K$-internal conversion coefficient, $\gamma$-ray angular distribution, $\gamma$-$\gamma$ coincidence, and $\gamma$-$\gamma$ angular correlation measurements. The results have led to an improved knowledge of the excitation energy pattern via the identification of new levels and transitions. New information on spin and parities of many levels as well as on mixing ratios of several transitions has been obtained. The presence of large $M1$ components in many transitions definitely excludes the possibility of considering $^{98}$Ru as a nucleus having a structure very close to the vibrational one and points to the need of an enlarged framework for a successful description.

DOI: 10.1103/PhysRevC.94.054327

## I. INTRODUCTION

The structure of the even ruthenium isotopes ($Z = 44$) changes from near spherical, for a neutron number close to $N = 50$, to $\gamma$ unstable, as $N$ increases. The isotopic chain has been extensively investigated both experimentally and theoretically. Particular attention has always been paid to the $^{98}$Ru isotope, the lighter member amenable to a collective description. Its excitation-energy pattern displays intriguing features owing to the presence of states of quite pure vibrational structure mixed with states that cannot be interpreted as members of phonon multiplets.

Such a puzzling behavior has stimulated the efforts of experimentalists to get more and more information on the spectroscopic properties of this nucleus. It has been studied using different reactions, properly suited to investigate specific properties. The results obtained along the years are summarized in Nuclear Data Sheets (NDS) [1]. Additional information on the properties of low-energy levels has been obtained in recent Coulomb excitation measurements [2–4], while a thorough study of the levels and decay scheme of $^{98}$Ru up to 6 MeV has been performed in Ref. [5].

In the past years different theoretical approaches have been considered [6–8] to reproduce the experimental data on the $^{98}$Ru isotope. Many studies have been performed in the framework of the interacting boson model [9]. In the IBA-1 version (which makes no distinction between proton and neutron bosons) it was found, since the first application of the model, that the $^{98}$Ru nucleus has a structure very close to that of the U(5) limit of the model (which corresponds to the vibrational model in a geometrical picture) as far as the study is limited to the yrast states up to $J = 8$ and to the states of the two-boson triplet. The possibility of describing $^{98}$Ru as a nucleus having a structure close to the $U_{\pi\nu}(5)$ limit of the IBA-2 model has been investigated in Refs. [10,11]. However, an extended comparison of experimental and calculated values was prevented by the lack of important spectroscopic data. To gain a deeper insight into the structure of this nucleus we have produced $^{98}$Ru via the $^{97}$Mo($^3$He,$2n$) reaction and have measured singles, internal electron conversion coefficients, $\gamma$ angular distributions, $\gamma$-$\gamma$ coincidences, and $\gamma$-$\gamma$ angular correlations.

Preliminary results have been reported in Ref. [12].

## II. EXPERIMENTAL METHODS AND RESULTS

The $^{98}$Ru nucleus was produced at the CN accelerator of Laboratori Nazionali di Legnaro (Padua) via the $^{97}$Mo($^3$He,$2n$) reaction, at a beam energy of 13 MeV and a typical current of 20 nA. The choice of the reaction was based on the requirement of populating both yrast and non-yrast states in a wide range of angular momenta. The beam energy was selected on the basis of our preliminary measurements of the excitation functions performed in the 12–13 MeV range.

Information on the $^{98}$Ru spectroscopic properties has been obtained through the measurements of single spectra, internal conversion coefficients, $\gamma$-ray angular distributions, $\gamma$-$\gamma$ coincidences, and $\gamma$-$\gamma$ angular correlations.

### A. Internal conversion coefficient measurements

In the measurements of $K$-conversion coefficients a self-supporting target (thickness of $\sim$1 mg/cm$^2$) was used, to avoid appreciable energy straggling of the emitted electrons. The total measuring time was about 55 hours. Internal conversion electrons were detected by means of a magnetic transport system [13] which deflects the electrons, emitted at 125° with respect to the beam direction, onto a 5 cm$^2$ × 6 mm Si(Li) detector cooled to liquid nitrogen temperature. The momentum acceptance of the system is $\Delta p/p = 18\%$ FWHM (full width at half maximum) and the energy resolution of the detector $\sim$2.2 keV for 1 MeV electrons. The area of electron lines, which have an asymmetric shape, was evaluated with a function resulting from the convolution with a Gaussian of a "delta" function plus an exponential "tail" on its low-energy side. The overall full energy peak efficiency is approximately constant at a value of about 1% over the 150–1200 keV energy range.

$\gamma$ rays were detected by a high-purity germanium (HPGe) detector, having 2.2 keV resolution (FWHM) at 1.3 MeV and 25% relative efficiency, placed 80 cm away from the target, at 55° with respect to the beam direction. Possible differences in the angular distributions of electron and $\gamma$ rays, which

 

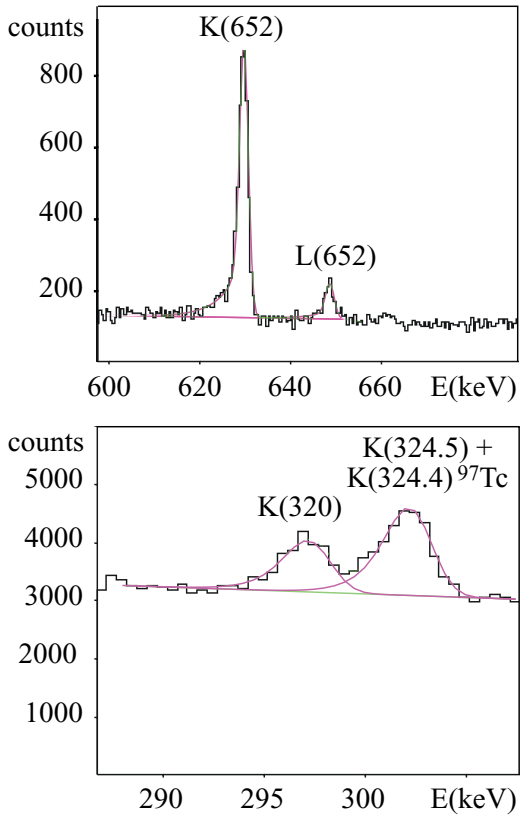


FIG. 1. Upper panel: $K$- and $L$-conversion lines of the 652.4 keV, $2_1^+ \rightarrow 0_1^+$ transition. Lower panel: $K$-conversion line (297.6 keV) of the 319.7 keV transition deexciting the 2867 keV level. It is clearly resolved from the doublet made up by the $K$-conversion lines (302.4 and 303.4 keV) of the 324.4 and 324.5 keV transitions of $^{98}$Ru and $^{97}$Tc, respectively.

would affect the final result, are strongly reduced at the angles selected for the Si and Ge detectors [$P_2 \cos(55^\circ) = 0$].

The energy and relative efficiency calibrations of the electron spectrometer were obtained using the internal conversion electrons from electron sources of $^{207}$Bi and $^{152}$Eu placed at the target position. The corresponding $\gamma$ rays provided the energy calibration for the germanium detector.

Energy spectra of electrons and $\gamma$ rays were simultaneously recorded by means of a multiplexed acquisition system. The signal from a high stability pulser was fed into each acquisition channel to allow corrections for dead time effects.

In order to check the effective source position (which affects the proportionality constant relating the magnetic field to the transmitted electron momentum) the $K$-conversion electrons of the 652.4 keV, $2_1^+ \rightarrow 0_1^+$ transition were recorded for different magnetic field settings and normalized to the corresponding $\gamma$ transition to determine the point of maximum transmission. Electron energy spectra were then recorded for several magnetic field settings corresponding to the maximum transmission of the electron lines of interest in the energy range 200–1000 keV. Examples of electron energy spectra are shown in Fig. 1.

Internal conversion coefficients were determined by means of the normalized peak-to-gamma (NPG) method [14], which refers to a transition of known multipolarity. The expression of the experimental $K$-conversion coefficient is given by

$$\alpha_K^{\exp}(E) = \frac{I_K(E)}{I_K(E_R)} \frac{\eta_e(E_R)}{\eta_e(E)} \frac{I_\gamma(E_R)}{I_\gamma(E)} \frac{\eta_{\text{gamma}}(E)}{\eta_\gamma(E_R)} \alpha_K(E_R).$$

Here $I_K$, $I_\gamma$ and $\eta_e$, $\eta_\gamma$ are the peak areas and the relative efficiencies of $K$-conversion and $\gamma$-ray lines at the energy of the transition of interest, $E$, and of the reference line, $E_R$.

The required normalization was provided by the 652.4 keV, pure $E2$ transition, recorded at the maximum of the transmission in the calibration run mentioned above.

For a few transitions connecting states of positive parity it has been possible to extract information on the absolute value of the $\delta(E2/M1)$ mixing ratio by comparing experimental and theoretical $\alpha_K$ values. The theoretical value is given by

$$\alpha_K = \frac{\alpha_K(M1) + \delta^2 \alpha_K(E2)}{(1+\delta^2)}.$$

The analysis results are summarized in Table I. The experimental $\alpha_K$ value of the 824.7 keV, $6_1^+ \rightarrow 4_1^+$ transition is reported to give an idea of the internal consistency of the data.

### B. Singles, $\gamma$ angular distribution, $\gamma$-$\gamma$ coincidence, and angular correlation measurements

In the measurements of singles, $\gamma$ angular distributions, and $\gamma$-$\gamma$ coincidences a 7.2 mg/cm$^2$ target of $^{97}$Mo (92% enriched) was used. A thin (100 $\mu$g/cm$^2$) gold layer was evaporated on the backside to reduce Doppler shift effects on the emitted radiation.

Angular distribution and $\gamma$-$\gamma$ coincidence measurements were performed by using an apparatus which employs five HPGe detectors mounted on a circular track, at adjustable angular positions and distances from the target. Cone shaped shields (internally copper lined) were utilized to define the acceptance of the detectors and to minimize $\gamma$ cross-scattering effects. In the present work the detectors were kept at fixed angles (60°, 110°, 215°, 270°, 315°) with respect to the beam direction, at a distance of 11 cm from the target. The layout of the apparatus is shown in Fig. 2. An additional HPGe detector, mounted on a vertical plane at 90° to the beam axis, at 27 cm from the beam line, provided singles spectra unaffected by Doppler shift effects. The detectors have a typical energy resolution of 2.3 keV at 1.33 MeV gamma energy and 25% relative efficiency. The energy calibration and detector efficiencies were obtained by using a $^{152}$Eu and a $^{56}$Co source at the target position. To perform an accurate energy calibration, in addition to the $\gamma$ lines of the two sources, we have also considered the $^{98}$Ru transitions reported by NDS with the uncertainty on the second decimal digit. The energy range was explored up to a maximum of about 2300 keV.

Angular distribution and $\gamma$-$\gamma$ coincidence measurements were carried out simultaneously, during three separate runs for a total acquisition time of about 80 hours. A pulser was used during the angular distribution measurements to correct for different dead times and possible gain changes.

In the $\gamma$-$\gamma$ coincidence experiment the resolving time was ~9 ns. The count rates of the detectors were such that differences among dead times could be neglected. For each

TABLE I. Experimental $K$-internal conversion coefficients, in units of $10^{-3}$ (column 5), are compared with the theoretical values [15] for $E1, E2, M1$, transitions (columns 5–7). The $J_i^\pi$ and $J_f^\pi$ spin parities of the initial and final states are from Ref. [1]. Previously reported $\alpha_K$ values are shown in column 9. The present results on parities are reported in column 10 and those on $|\delta|$ in column 11. The upper limit for $|\delta|$ of the 253.8 keV transitions is given at 95% confidence level. The presence of an unresolved and very weak (as detected in $\gamma$-$\gamma$ measurements) 879.5 keV (1144.2 keV) transition from the 2276.8 keV (4213.8 keV) level does not affect the $\alpha_K^{\rm exp}$ value of the 879.2 keV (1144.5 keV) transition.

| $E_{\rm lev}$ (keV) | $J_i^\pi$ | $E_\gamma$ (keV) | $J_f^\pi$ | $\alpha_K^{\rm exp}$ | $\alpha_K$ ($E1$) | $\alpha_K$ ($E2$) | $\alpha_K$ ($M1$) | Ref. [16] | $J_i^\pi$ | $\lvert\delta\rvert$ |
|---|---|---|---|---|---|---|---|---|---|---|
| 1797.0 | $3^+$ | 382.7 | $2^+$ | 9.0(8) | | 10.5 | 7.8 | | | $0.9^{+0.8}_{-0.5}$ |
| | | 1144.5 | $2^+$ | 0.65(15) | | 0.575 | 0.627 | 0.7(3) | | |
| 1817.2 | $(2)^+$ | 1164.8 | $2^+$ | 1.0(3) | | 0.554 | 0.604 | | | |
| 2222.5 | $6^+$ | 824.7 | $4^+$ | 1.29(9) | | 1.22 | | 1.2(2) | | |
| 2266.5 | $4^+$ | 253.8 | $3^+$ | 20(2) | | 40.5 | 22.0 | | | $<0.35$ |
| 2276.8 | $(2^+)$ | 879.2 | $4^+$ | 0.80(29) | 0.428 | 1.05 | 1.13 | 1.4(3) | $(2)^+$ | |
| 2867.3 | $(6^+)$ | 320.3 | $(5,6)^+$ | 12.3(12) | 4.55 | 18.5 | 12.2 | | $(6)^+$ | 0.0(5) |
| | | 644.8 | $6^+$ | 2.44(52) | 0.821 | 2.28 | 2.24 | | | |
| 3069.2 | | 846.6 | $6^+$ | 1.36(30) | 0.462 | 1.15 | 1.21 | | $4^+ - 8^+$ | |
| 3190.2 | $(8^+)$ | 967.7 | $6^+$ | 0.84(20) | 0.355 | 0.835 | 0.901 | 0.9(3) | $(8)^+$ | |
| 3245.2 | $(6^+)$ | 978.8 | $4^+$ | 0.81(27) | 0.347 | 0.814 | 0.878 | | $(6)^+$ | |
| 3250.6 | | 984.4 | $4^+$ | 1.22(38) | 0.343 | 0.803 | 0.868 | | $2^+ - 6^+$ | |
| 3283.3 | $(7)^-$ | 1060.6 | $6^+$ | 0.90(25) | 0.298 | 0.679 | 0.738 | 0.23(10) | $(7)^+$ | |
| 3538.5 | $(6^+,7,8^+)$ | 991.8 | $(5,6)^+$ | 0.97(48) | 0.339 | 0.790 | 0.854 | | | |

coincidence event involving at least two Ge detectors the $\gamma$-ray energies and the time interval between the signals from the detectors were collected and stored on magnetic tape for offline analysis. Altogether about $4.3 \times 10^8$ events were stored.

#### *1. Singles and γ-γ coincidence analysis*

The information obtained from both singles and $\gamma$-$\gamma$ coincidences has been used to achieve an improved knowledge of the decay scheme of $^{98}$Ru nucleus and to evaluate the relative intensity of the transitions deexciting the levels.

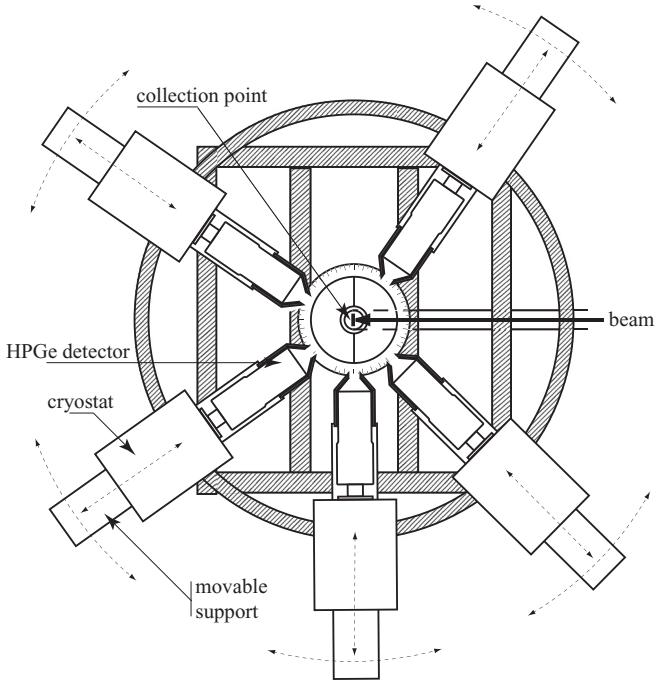


FIG. 2. Schematic view of the apparatus utilized in angular distribution and correlation measurements.

To improve the statistics and reduce angular correlation effects on the relative intensities of $\gamma$ lines, the coincidence spectra of the five detectors, gated on a given transition and properly corrected for different energy calibrations, were summed up. Several new levels and gamma transitions have been identified.

As an example of the procedure followed in the analysis, we consider the case of a multiplet of three transitions found at an energy of $\simeq$ 1722 keV. To this aim we show in Fig. 3 the relevant sections of the spectra gated on (a) the 652.4 keV, $2_1^+ \rightarrow 0_1^+$, (b) the 745.4 keV, $4_1^+ \rightarrow 2_1^+$, (c) the 824.7 keV, $6_1^+ \rightarrow 4_1^+$ keV transitions, and on (d) a small energy region centered at $\simeq$ 1722 keV. Clearly, the different intensities of the 652.4, 745.4, and 824.7 keV transitions in panel (d) point to the presence of closely spaced transitions feeding the $2_1^+$, $4_1^+$, and $6_1^+$ levels. By proper subtraction of the spectra in panels (a), (b), and (c) we established the energies of a triplet of $\gamma$ lines of 1719.2, 1722.4, and 1721.9 keV. They deexcite the levels at 2371, 3120, and 3944 keV to the $2_1^+$, $4_1^+$, and $6_1^+$ states, respectively. A single transition of 1722(1) keV from a level at 2374.5 was reported by NDS while only a 1723.1 keV transition from the 3946.4 keV level to the $6_1^+$ state was reported by Cakirli *et al.* [5].

Following a similar procedure for the peak marked by the left arrow in panels (a) and (b), we infer the existence of two transitions having energies of 1710.1 and 1710.7 keV, which deexcite the 2362 and 3120 keV levels to the $2_1^+$ and $3_2^+$ states, respectively. The right arrow marks a 1734.6 keV transition, which connects the 3132 keV level to the $4_1^+$ state. None of the levels just mentioned was previously identified.

Spectra concerning the identification of the new levels at 2670 and 2707 keV, which deexcite to the $2_2^+$ state via the 1256.1 and 1293.0 keV transitions, respectively are presented

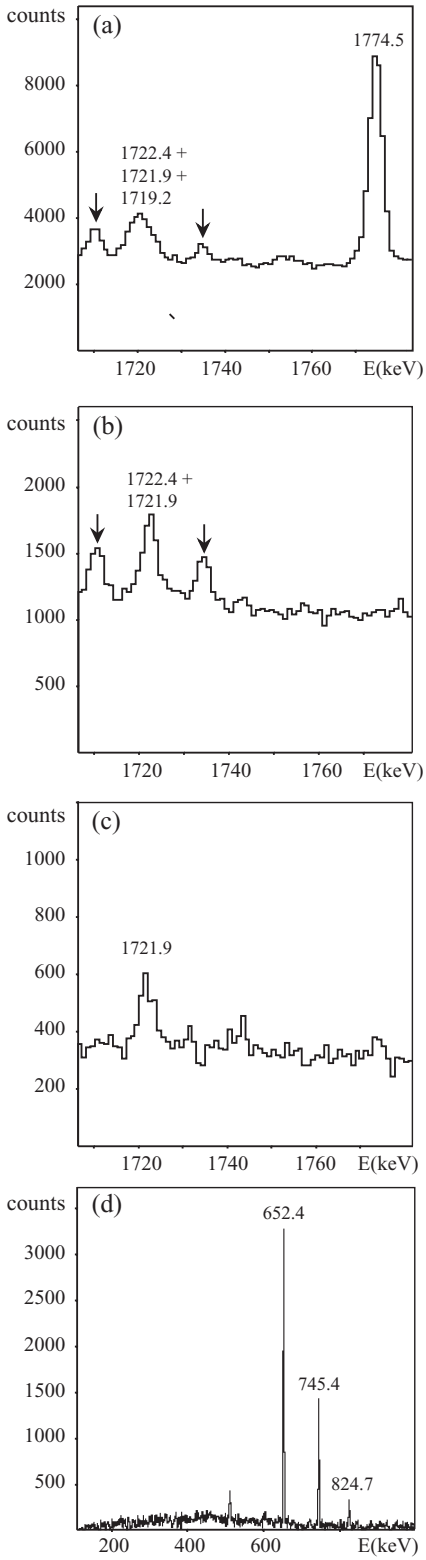


FIG. 3. Partial energy spectra obtained by gating on (a) the $2_1^+ \rightarrow 0_1^+$, 652.4 keV, (b) $4_1^+ \rightarrow 2_1^+$, 745.4 keV, (c) $6_1^+ \rightarrow 4_1^+$, 824.7 keV transitions and on (d) a small region around 1722 keV. The 1774.5 keV transition deexciting the 2427 keV level is shown to give an idea of the FWHM of the lines in this energy region. The arrows in panels (a) and (b) mark the presence of new transitions found in this work (see text per detail).

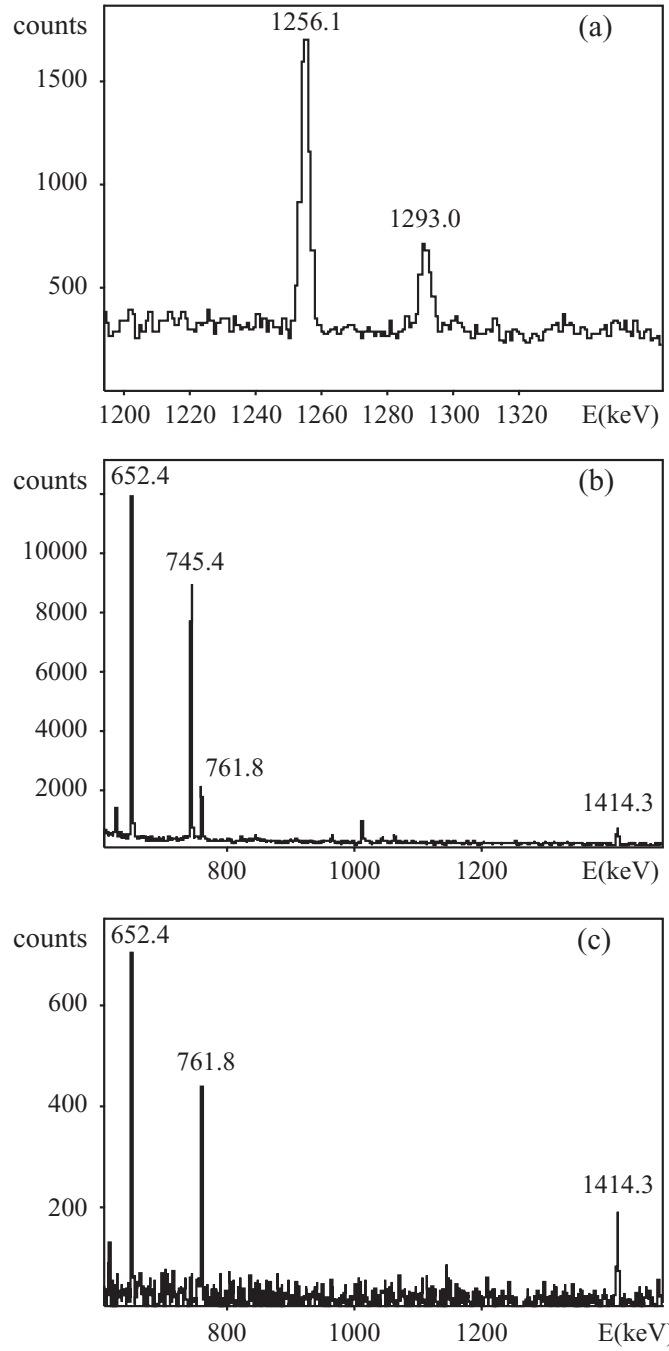


FIG. 4. (a) Section of the $\gamma$ energy spectrum obtained by gating on the 761.8, $2_2^+ \rightarrow 2_1^+$ keV transition. The 1256.1 and 1293.0 keV transitions deexcite the 2670 and 2707 keV levels, respectively. (b), (c) Section of the $\gamma$ energy spectrum obtained by gating on (b) a region around 1256–1258 keV and (c) the 1293.0 keV transition. The presence in panel (b) of the 745.4 keV transition is due to decay of the 2656 keV level to the $4_1^+$ state via the 1258.7 keV transition.

in Fig. 4. In this example the identification of the levels is straightforward.

The relative intensity of the transitions deexciting a given level has been evaluated, when possible, in both singles and coincident spectra. As a final value we adopted the weighted

average of the two data, when compatible. The existence of a significant difference between the two evaluations has been considered as indicative of the presence of contaminants. As an example, we mention the case of the intensity ratio of the 324.4 and 1149.2 keV transitions, deexciting the 2547 keV level. Its value in singles is much larger than in the coincidences spectra gated on the transitions which populate the 2547 keV level. The contaminant has been identified as a transition deexciting the 324.5 keV state to the ground state, of $^{97}$Tc [17], produced via ($^{3}$He , $pn$) reaction on $^{96}$Mo, present at the 2% level in the target.

It must be stressed that, because of the limited energy range we have explored (up to about 2300 keV), transitions deexciting states of energy larger that $\simeq 3$ MeV in coincidence with the $2_1^+ \rightarrow 0_1^+$ transition cannot be observed. The loss of transitions towards low-lying states increases for increasing energies. Because of the spin values of the the low-lying levels the missed states have predominantly low spins.

The results of the present work on level energies, $\gamma$ transitions and intensity ratios are summarized in columns 7–9 of Table II. Here, they are compared with the data reported by NDS (states of unknown decay have not been considered) and by Cakirli *et al.* [5] in columns 1–3 and 4–6, respectively.

Hereafter we comment on some specific cases.

*1322 keV level.* Cakirli *et al.* [5] are doubtful about the consistence of their results on the transition of 670 keV deexciting this level to the $0_1^+$ state with those reported in the literature. In singles we observe a doublet at about 670 keV. In the gate on the 652.4 keV only a 669.9(1) keV line is present. A 670.3(2) keV line is observed in the spectrum gated on the 324.4 keV transition which, as mentioned above, contains a strong component due to $^{97}$Tc nucleus [17]. It has been identified as the 670.21 keV transition connecting the 994 keV state to the 324 keV one in this nucleus.

*1817 keV level.* A transition deexciting this level to the $0_1^+$ state is reported by NDS. It is very doubtful for Cakirli *et al.* [5] who, in fact, consider the spin-parity $J^\pi = 0^+$ as possible for this state. The transition is clearly observed in the present work in the spectrum gated by the 610.0 keV transition, populating the 1817 keV state from the 2427 keV level.

*1953 keV level.* A level at 1953 keV was tentatively proposed by Samudra *et al.* [6] on the basis of a 1301 keV transition to the $2_1^+$ state. Cakirli *et al.* [5] found no evidence of this transition and consequently of this level. We observe a 1301.2 keV $\gamma$ ray in the spectra gated by the 652.4, 745.4, and 824.7 keV transitions and assigned this transition to a new level at 3524 keV level, thus definitely excluding the existence of the 1953 keV level.

*2277 keV level.* A 879.2 keV transition deexcites this level to the $4_1^+$ state. It is part of an unresolved doublet which contains also the 879.5 keV transition connecting the 4006 keV level to the $8_1^+$ state. The difficulty in evaluating separately each transition is probably the cause of the noticeable disagreement between Ref. [1] and Ref. [5] about the relative intensities of the 879.2 and 1624.2 transitions from the 2277 keV state and of the 879.5 and 722.4 keV transitions from the 4006 keV state. To obtain a reliable estimate of the relative intensities of the two member of the doublet we followed a procedure analogous to that described above for the transitions of $\simeq$1722 keV. We found that the intensity of the 879.5 keV deexciting the 4006 keV level, is only $\simeq$4% that of 879.2 keV transition. This implies a negligible correction for the measured internal conversion coefficient of the 879.2 keV transition (see Table I).

*2468 keV level.* According to NDS this level deexcites via the 670.2 and 2467.6 keV transitions. In agreement with Ref. [5] we do not observe the 670.2 keV transition. We cannot check the existence of the transition to the $0_1^+$ state because its energy is outside the energy range investigated; however, the identification of the 1815.9 keV transition to the $2_1^+$ level confirms the existence of this state.

*2547 keV level.* The identification of a new transition of 534.2 keV deexciting this level to the $3_2^+$ state proves to be essential for the $J^\pi$ assignment to this state.

*2670 keV level.* Evidence of the existence of this state is presented in Fig. 4. It is probably to be associated to that observed at 2671(10) keV by Du Marche' *et al.* [16] in the $(p,p')$ reaction.

*3069 keV doublet.* A doublet of 3069.3 and 3069.4 keV levels is reported in Ref. [1]. The first level decays via a 522 and a 847 keV transition, the second one via a 2417 keV transition. Reference [5] report only a level at 3070.3 keV, decaying via a 522.5 keV transition. We observe both the transitions reported by NDS for the 3069.3 keV level, but are not able to check the existence of the 3069.4 keV level, because the 2417 keV transition falls outside our recorded energy range.

*3851 keV level.* Our findings about the transitions deexciting this level considerably differ from the data reported in the literature, except for the transition connecting this state to the $8_1^+$ state. For this transition we measured an energy of 724.7(1) keV, which implies an energy of the state of 3851.0(1). From the analysis of different gates we can exclude the assignment of the 272 keV transition to the decay of the 3851 keV level; however, its placement in the decay scheme remains unassigned. The 312 keV transitions, reported in Refs. [1,5] as de-exciting this level to the 3538 keV levels, is not observed in the present work.

Reference [1] reports a 567.4 keV transition deexciting the 3851 keV level to the $8_2^+$ state; Refs. [1,5] report a 661.3 keV transition to the $8_1^+$ state. The energies we found for these transitions are 569.0(2) and 662.1(4) keV, respectively. Adding these energies to those (known very precisely) of the $8_2^+$ and $8_1^+$ states, respectively, we have ascertained the existence of a new level at 3852.5(2). We finally remark that the energies of the 272.2, 312.7, and 567.4 keV transitions are given without errors by NDS.

*4006 keV level.* Reference [5] reports two levels, very close in energy, at 4006.6 and 4007.4 keV. An accurate check of the energies of the transitions deexciting these levels leads to the conclusion that only one level exists (at 4005.7 keV), in agreement with Ref. [1].

*4223 keV level.* Two levels, at 4221.7 and 4224.7 keV, which deexcite to the 3191 keV level via 1030.4 and 1033.3 keV transitions, respectively, are reported in Ref. [5]. We observe only a 1032.5 keV transition in the gate on the 967.7 keV transition, which deexcites the 3190 keV level. The existence of the 4221.7 keV level, based only on the presence of the 1030.4 keV transition, is therefore not confirmed.

TABLE II. Level and $\gamma$-transition energies (in keV) reported in Refs. [1] and [5] are shown in columns 1–2 and 4–5, respectively. In columns 1 and 2 energies are given without errors when the uncertainty is on the second decimal digit. The branchings of Ref. [1] and those deduced in the present work from Table I of Ref. [5] are shown in columns 3 and 6, respectively. In Ref. [5] the uncertainties on the energies range from 0.2 keV for the stronger transitions to 0.4 keV for the weaker ones; analogously, those on the relative intensities range from 1% to 5–15%, respectively. The results of the present work are shown in columns 7–9. In columns 7 and 8 the energies reported without errors are taken from Ref. [1]. Transitions that in Ref. [1] or [5] are placed differently than in the present work are marked by a superscript *a*. New levels are shown in boldface characters and levels previously observed in only one of Refs. [1] and [5] are marked by a star. The main gates on which the present placement of new transitions (or observed only in Ref. [1] or [5]) is based are given in column 10. Transitions having an energy larger than 2.3 MeV are marked by the symbol **ne** (not evaluated) because they are outside the energy range recorded in the experiment.

| $E_i$ | $E_\gamma$ | $I_\gamma$ | $E_i$ | $E_\gamma$ | $I_\gamma$ | $E_i$ | $E_\gamma$ | $I_\gamma$ | Gates |
|---|---|---|---|---|---|---|---|---|---|
| 652.44 | 652.43 | 100 | 652.6 | 652.6 | 100 | 652.44 | 652.43 | 100 | |
| 1322.14 | 669.70 | 100 | 1320.7 | 668.1 | 100 | 1322.14 | 669.70 | 100 | |
| 1397.82 | 745.36 | 100 | 1398.2 | 745.6 | 100 | 1397.82 | 745.36 | 100 | |
| 1414.29 | 761.84 | 100(1) | 1414.9 | 762.3 | 100 | 1414.29 | 761.84 | 100(2) | |
| | 1414.29 | 50(1) | | 1415.0 | 49 | | 1414.29 | 49(1) | |
| 1796.96 | 382.65 | 26(1) | 1797.6 | 382.7 | 26 | 1796.96 | 382.65 | 27(3) | |
| | 399.1(3) | 7(1) | | 399.1 | 7 | | 398.8(2) | 10(3) | |
| | 1144.52 | 100(7) | | 1145.1 | 100 | | 1144.52 | 100(1) | |
| 1817.22 | | | 1817.9 | | | 1817.22 | 494.7(3) | 3(1) | 670 |
| | 1164.78 | 100(7) | | 1165.3 | 100 | | 1164.78 | 100(5) | |
| | 1817.4(5) | 38(3) | | 1818.4 | 14 | | 1817.1(3) | 18(3) | |
| 1953.4?(3) | 1301.0(3)[a] | 100 | | | | | | | |
| 2012.70 | 598.44 | 92(11) | 2013.4 | 598.9 | 89 | 2012.70 | 598.44 | 70(4) | |
| | 614.87 | 100(13) | | 615.0 | 100 | | 614.87 | 100(4) | |
| | 1360.9(5) | 17(3) | | 1360.9 | 10 | | 1360.1(4) | 6(1) | |
| 2222.51 | 824.69 | 100 | 2223.3 | 825.1 | 100 | 2222.51 | 824.69 | 100 | |
| 2241.4?(3) | 843.6(3) | 100 | | | | 2241.4(5) | 843.6(5) | 100 | 652, 745 |
| 2245.9(3) | 1593.4(3) | 100 | 2246.0 | 1593? | | 2245.8(2) | 1593.4(2) | 100 | 652 |
| | | | | | | 2257.8(4) | 843.5(4) | 100 | 762, 1414 |
| 2266.50 | 253.80 | 22(2) | 2267.2 | 253.8 | 26 | 2266.50 | 253.80 | 20(3) | |
| | 469.54 | 100(8) | | 469.6 | 100 | | 469.54 | 100(3) | |
| | 868.7(3) | 26(4) | | 869.2 | 29 | | 868.4(2) | 30(3) | |
| 2276.8(3) | | | 2278.0 | | | 2276.8(2) | 264.1(4) | 5(1) | 598, 615 |
| | 879.0(3) | <56 | | 879.6 | 92 | | 879.2(1) | 57(3) | |
| | 1624.3(3) | 100(25) | | 1625.4 | 100 | | 1624.2(3) | 100(4) | |
| | | | | | | **2295.4(2)** | 897.6(2) | 100 | 652, 745 |
| | | | | | | **2362.5(3)** | 1710.1(3) | 100 | 652 |
| 2374.5(10) | | | 2374.0? | | | 2371.3(2) | 956.7(3) | 14(4) | 762, 1414 |
| | 1722(1) | | | | | | 1719.2(3) | 100(10) | 652 |
| | | | | | | **2406.1(2)** | 991.7(2) | 48(10) | 762, 1414 |
| | | | | | | | 1084.1(2) | 64(6) | 652, 670 |
| | | | | | | | 1753.5(3) | 100(16) | 652 |
| 2427.1(2) | 610.1(3) | 9(2) | 2427.9 | 609.9 | 7 | 2426.9(1) | 610.0(1) | 10(1) | |
| | 630.1(3) | 7(2) | | 630.3 | 6 | | 629.8(2) | 11(1) | |
| | | | | | | | 1012.7(1) | 11(1) | 652, 762 |
| | 1029.4(3) | 18(5) | | 1029.7? | <20 | | 1029.0(1) | 21(1) | |
| | 1774.5(3) | 100(11) | | 1776.4 | 100 | | 1774.5(3) | 100(2) | |
| 2430.2?(3) | 1032.4(3)[a] | | | | | | | | |
| 2467.6(10) | 670.2(7) | 100(10) | | | | 2468.3(2) | | | |
| | | | | | | | 1815.9(2) | 100 | 652 |
| | 2467.6 | 19.5(24) | | | | | **ne** | | |
| 2473.8?(5) | 197.0(3) | | | | | | | | |
| 2546.99 | | | 2547.8 | 280.5 | 5 | 2546.99 | 280.5(2) | 10(2) | 320, 470 |
| | 324.5(3) | 22(2) | | 324.6 | 22 | | 324.4(1) | 20(2) | |
| | | | | | | | 534.2(2) | 11(3) | 320, 615 |
| | 1149.17 | 100(9) | | 1149.7 | 100 | | 1149.17 | 100(4) | |
| 2602.3(3) | | | 2603.5 | | | 2602.2(1) | 325.2(3) | 23(4) | 879, 1624 |
| | 591(1) | 75(25) | | 589.6 | 52 | | 589.5(2) | 100(7) | |
| | | | | | | | 785.3(3) | 12(3) | 1165 |
| | | | | | | | 1188.0(3) | 39(5) | 762, 1414 |

TABLE II. (*Continued.*)

| $E_i$ | $E_\gamma$ | $I_\gamma$ | $E_i$ | $E_\gamma$ | $I_\gamma$ | $E_i$ | $E_\gamma$ | $I_\gamma$ | Gates |
|---|---|---|---|---|---|---|---|---|---|
| | 1204.4(3) | 100(50) | | 1205.7 | 100 | | 1204.4(2) | 67(5) | |
| | | | | | | | 1949.1(10) | 40(18) | 652 |
| 2619.8(5) | | | | | | 2619.5 (3) | 802.2(4) | 10(2) | 1165 |
| | 1967.3(5) | 100(9) | | | | | 1967.2(5) | 100(7) | 652 |
| | 2619.2 | 11.7(12) | | | | | **ne** | | |
| 2656.52 | | | 2657.5 | | | 2656.52 | 643.9(2) | 6(1) | 598, 615 |
| | 1258.69 | 100 | | 1259.3 | 100 | | 1258.69 | 100(2) | |
| 2659.62 | 862.66 | 100 | 2660.8 | 863.2 | 100 | 2659.62 | 862.66 | 100 | |
| | | | | | | **2670.4(2)** | 853.2(2) | 12(2) | 652, 1165 |
| | | | | | | | 1256.1(5) | 100(4) | 652, 762 |
| | | | | | | | 2018.1(7) | 14(3) | 652 |
| | | | | | | **2707.2(3)** | 889.7(4) | 10(3) | 1165 |
| | | | | | | | 1293.0(2) | 100(16) | 652, 762 |
| | | | | | | | 1385.6(4) | 12(3) | 652, 670 |
| 2720.3(3) | 1322.5(3) | 100 | 2720.4 | 1322.2 | 100 | 2720.0(1) | 1322.2(1) | 100(3) | |
| | | | | | | | 2068.1(5) | 11(2) | 652 |
| | | | | | | **2754.2(3)** | 937.0(3) | 100 | 1165, 1817 |
| | | | 2786.6 | 563.3 | 100 | | | | |
| 2809.2(2) | 542.7(3) | 100(33) | 2810.0 | 542.8 | 100 | 2809.3(1) | 542.8(1) | 95(5) | |
| | | | | | | | 796.4(2) | 19(2) | 598, 615 |
| | 1012.2(3) | 78(22) | | | | | 1012.4(1) | 100(8) | 762, 1145 |
| | | | | | | | 1411.5(5) | 33(8) | 652, 745 |
| | | | | | | **2811.5(3)** | 1397.2(3) | 100(7) | 762, 1414 |
| | | | | | | | 1413.7(4) | 58(10) | 652, 745 |
| | | | | | | **2816.6(2)** | 999.3(4) | 17(4) | 1165 |
| | | | | | | | 1402.2(4) | 33(8) | 762, 1414 |
| | | | | | | | 1418.9(3) | 100(11) | 652, 745 |
| | | | | | | | 2164.4(6) | 91(15) | 652 |
| | | | | | | **2825.8(2)** | 1428.0(2) | 100 | 652, 745 |
| | | | | | | **2859.1(2)** | 846.4(2) | 100 | 598, 615 |
| 2867.7(2) | 320.7(3) | 100(18) | 2868.4 | 320.6 | 100 | 2867.3(1) | 320.3(1) | 100(5) | |
| | 645.2(3) | 45(9) | | 645.1 | 16 | | 644.8(2) | 52(3) | |
| | | | | | | | 1469.2(4) | 8(2) | 745 |
| | | | | | | **2932.6(2)** | 710.0(2) | 62(13) | 745, 824 |
| | | | | | | | 2280.8(6) | 100(27) | 652 |
| | | | | | | **2954.3(3)** | 527.4(3) | 100 | 610, 1774 |
| | | | | | | **2979.7(7)** | 1675.6(7) | 100 | 670 |
| | | | | | | **3014.4(6)** | 1616.6(6) | 100 | 652, 745, |
| | | | | | | **3016.8(3)** | 1619.0(3) | 100 | 652, 745 |
| | | | | | | **3026.6(5)** | 1013.9 (5) | 100 | 598, 615 |
| | | | 3058.7 | 835.4 | 100 | | | | |
| 3064.9(3) | | | 3066.7 | | | 3064.8(1) | 408.3(2) | 7(1) | 745, 1258 |
| | | | | | | | 1052.1(2) | 10(3) | 598, 615 |
| | 1667.1(3) | 100 | | 1668.5 | 100 | | 1667.0(1) | 100(4) | |
| 3069.3(7) | 522(1) | 29(15) | 3070.3 | 522.5 | 100 | 3069.2(2) | 522.2(2) | 9(1) | |
| | 847(1) | 100(29) | | | | | 846.6(3) | 100(6) | 745, 824 |
| | | | | | | | 1671.0(3) | 12(1) | 652, 745 |
| 3069.4(11) | 2417(1) | 100 | | | | | **ne** | | |
| | | | | | | **3074.6(2)** | 418.3(2) | 55(6) | 745,1258 |
| | | | | | | | 1061.7(3) | 45(9) | 598, 615 |
| | | | | | | | 1676.7(2) | 100(12) | 652, 745 |
| | | | | | | **3093.7(3)** | 1679.6(4) | 51(16) | 762 |
| | | | | | | | 1695.7(5) | 100(18) | 652, 745 |
| | | | | | | **3097.5(2)** | 1699.7(2) | 100 | 652, 745 |
| | | | | | | **3109.1(2)** | 452.3(3) | 16(3) | 745, 1258 |
| | | | | | | | 682.2(2) | 100(8) | 610, 1774 |
| | | | | | | | 1312.3(2) | 46(7) | 652, 1145 |
| | | | | | | | 1710.7(3) | 73(4) | 652, 745 |

TABLE II. (*Continued*.)

| $E_i$ | $E_\gamma$ | $I_\gamma$ | $E_i$ | $E_\gamma$ | $I_\gamma$ | $E_i$ | $E_\gamma$ | $I_\gamma$ | Gates |
|---|---|---|---|---|---|---|---|---|---|
| | | | | | | **3120.2(2)** | 1107.6(3) | 28(7) | 598, 615 |
| | | | | | | | 1722.4(2) | 100(8) | 652, 745 |
| 3126.31 | 903.80 | 100 | 3127.4 | 904.1 | 100 | 3126.31 | 903.80 | 100 | |
| | | | | | | **3132.5(3)** | 476.2(5) | 8(2) | 1258 |
| | | | | | | | 1734.6(3) | 100(5) | 652, 745 |
| 3178.8(6) | 1764.6 | 9(1) | | | | **ne** | | | |
| | 2526.1 | 100(7) | | | | | **ne** | | |
| | 3179.3 | 50(5) | | | | | **ne** | | |
| | | | | | | **3184.9(1)** | 638.0(2) | 48(4) | 324,745,1149 |
| | | | | | | | 962.3(2) | 43(3) | 745, 824 |
| | | | | | | | 1172.2(1) | 100(5) | 598, 615 |
| 3190.20 | 967.69 | 100 | 3191.3 | 968.0 | 100 | 3190.20 | 967.69 | 100 | |
| 3205.5(8) | | | | | | 3205.2(3) | 1388.5(6) | 50(15) | 1165 |
| | 1792.3 | 63(18) | | | | | 1790.6(4) | 72(21) | 762,1414 |
| | | | | | | | 1807.2(6) | 100(20) | 745 |
| | 2552.3 | 100(11) | | | | | **ne** | | |
| 3245.4(3) | | | 3246.4 | | | 3245.2(1) | 698.1(2) | 12(2) | 745, 1149 |
| | 978.9(3) | 100 | | 979.2 | 100 | | 978.8(1) | 100(4) | |
| | | | | | | | 1022.3(2) | 15(2) | 745, 824 |
| 3250.9(3) | | | 3252.1 | 591.3 | 46 | 3250.6(2) | 590.7(2) | 38(4) | 862, 1145 |
| | | | | 594.7 | 56 | | 594.2(2) | 42(5) | 745, 1258 |
| | 984.4(3) | 100 | | 984.9 | 100 | | 984.4(2) | 100(6) | |
| | | | | | | **3279.2(2)** | 1482.2(5) | 43(12) | 1145 |
| | | | | | | | 1881.4(2) | 100(6) | 652, 745 |
| 3283.5(2) | 626.9(3) | 29(4) | 3284.5 | 627.1 | 26 | 3283.3(1) | 626.9(1) | 24(2) | |
| | 1060.9(3) | 100(10) | | 1061.2 | 100 | | 1060.6(1) | 100(2) | |
| | | | | | | **3287.9(2)** | 1065.4(2) | 100 | 745, 824 |
| | | | | | | **3350.4(3)** | 1084.0(3) | 61(12) | 470, 1145 |
| | | | | | | | 1553.0(5) | 100(22) | 652, 1145 |
| | | | | | | **3382.8(2)** | 1106.0(3) | 58(11) | 879, 1624 |
| | | | | | | | 1370.0(4) | 48(14) | 598,615 |
| | | | | | | | 1585.9(4) | 100(28) | 652, 1145 |
| 3441.3(6) | | | | | | 3442.1(3)* | 1014.8(3) | 42(12) | 1774 |
| | 1428.1(5) | 79(7) | | | | | | | |
| | 1624.7(6) | 100(11) | | | | | 1625.3(5) | 22(4) | 1165 |
| | | | | | | | 2045.1(5) | 100(8) | 652, 745 |
| | | | 3476.4 | 229.8 | 66 | 3474.7(2)* | 229.1(2) | 78(13) | 470, 979 |
| | | | | 1253.2 | 100 | | 1252.3(2) | 100(13) | 745, 824 |
| | | | | | | | 2076.5(5) | 96(21) | 652, 745 |
| | | | | | | **3523.5(2)** | 803.0(4) | 11(3) | 1322 |
| | | | | | | | 1301.2(2) | 100(6) | 745, 824 |
| 3538.4(2) | 412.1(3) | 81(6) | 3539.8 | 412.4 | 100 | 3538.5(1) | 412.1(1) | 100(6) | |
| | 991.4(3) | 100(13) | | 992.0 | 79 | | 991.8(2) | 65(5) | |
| | | | | | | **3562.1(3)** | 1014.9(3) | 69(13) | 1149 |
| | | | | | | | 1340.0(4) | 100(11) | 745, 824 |
| 3579.7(5) | 295.1 | | 3579.9 | 295.5 | 26 | 3578.5(1) | 295.0(2) | 19(4) | |
| | 1033.7 | | | 1032.1 | 100 | | 1031.5(1) | 100(7) | |
| | 1357.6 | | | | | | 1356.1(4) | 15(3) | 745, 824 |
| | | | | | | **3620.4(2)** | 1397.9(2) | 100 | 745, 824 |
| | | | | | | **3623.9(2)** | 967.4(2) | 100 | 745,1258 |
| | | | | | | **3637.7(3)** | 1415.2(3) | 100 | 745, 824 |
| | | | | | | **3671.1(2)** | 1014.6(2) | 100 | 745,1258 |
| | | | | | | **3703.1(2)** | 1046.6(2) | 100 | 745, 1258 |
| | | | | | | **3721.8(2)** | 438.5(3) | 46(9) | 824, 1061 |
| | | | | | | | 1065.2(2) | 100(10) | 745, 1258 |
| 3851.6(2) | 272.2 | 4 | 3852.6 | 272.8 | 4 | 3851.0(1) | | | |
| | 312.7 | 4 | | 312.7 | 3 | | | | |
| | 567.4[a] | 2 | | | | | | | |

TABLE II. (*Continued.*)

| $E_i$ | $E_\gamma$ | $I_\gamma$ | $E_i$ | $E_\gamma$ | $I_\gamma$ | $E_i$ | $E_\gamma$ | $I_\gamma$ | Gates |
|---|---|---|---|---|---|---|---|---|---|
| | 661.3(4)[a] | 4 | | 661.3[a] | 3 | | | | |
| | 725.4(3) | 100 | | 725.2 | 100 | | 724.7(1) | 100 | |
| | | | | | | **3852.5(2)** | 569.0(2) | 100(23) | 824, 1061 |
| | | | | | | | 662.1(4) | 51(16) | 824, 967 |
| | | | 3857.1 | 317.3 | 100 | 3854.9(2)* | 316.4(1) | 100(19) | 904, 992 |
| | | | | | | | 987.6(5) | 71(16) | 320, 645 |
| | | | 3946.4 | 1723.1 | 100 | 3944.4(2)* | 1721.9(2) | 100 | 745, 824 |
| | | | | | | **3964.8(4)** | 1742.3(4) | 100 | 745, 824 |
| | | | | | | **3971.7(2)** | 1301.5(3) | 70(11) | 762, 1256 |
| | | | | | | | 1315.7(4) | 64(12) | 745, 1258 |
| | | | | | | | 1958.4(4) | 100(20) | 598, 615 |
| 4001.3(3) | 810.9(4) | 46(4) | 4002.1 | 810.7 | 43 | 4000.6(1) | 810.3(2) | 38(4) | |
| | 875.1(4) | 100(8) | | 874.7 | 100 | | 874.3(1) | 100(7) | |
| 4006.0(3) | 722.5(3) | 100(8) | 4006.6 | | | 4005.7(1) | 722.4(2) | 100(8) | |
| | | | | 754.5 | 100 | | 754.3(2) | 48(15) | 470, 984 |
| | | | | | | | 815.4(2) | 51(4) | 824, 978 |
| | 879.8(4) | 85(7) | | | | | 879.5(2) | 43(5) | |
| | | | 4007.4 | 722.9[a] | 100 | | | | |
| | | | | 816.1[a] | 46 | | | | |
| | | | | 879.6[a] | 32 | | | | |
| | | | 4135.7 | 889.3 | 100 | 4134.7(3)* | 889.3(3) | 100 | 470, 978 |
| | | | 4216.1 | 214.3 | 44 | 4213.7(2)* | | | |
| | | | | 1024.9 | 100 | | 1023.5(3) | 24(4) | 824, 967 |
| | | | | 1088.5 | 61 | | | | |
| | | | | | | | 1144.6(3) | 100(8) | 824, 847 |
| | | | 4221.7 | 1030.4 | 100 | | | | |
| 4223.3(3) | 1033.2(4) | 100(7) | 4224.7 | 1033.3 | 100 | 4222.8(2) | 1032.5(2) | 100(10) | |
| | 1096.9(4) | 85(7) | | 1097.5 | 49 | | 1096.9(4) | 33(9) | |
| | | | 4258.5 | 1012.1 | 100 | 4256.2(3)* | 1011.0(3) | 100 | 470, 978 |

#### 2. *Angular distributions analysis*

The angular distribution of a $\gamma$ ray emitted from an oriented state can be described as [18]

$$W(\theta) = A_{00}[1 + Q_2 A_{22}(\gamma) P_2(\cos\theta) + Q_4 A_{44}(\gamma) P_4(\cos\theta)],$$

where $Q_k$ are solid-angle correction factors and $P_k$ the Legendre polynomials. The angular distribution coefficients $A_{kk}$ can be expressed as the product of orientation parameters $B_k(J)$, which describe the alignment (relative population of the magnetic substates) of the initial state of spin $J = J_i$, and coefficients $A_k(\lambda)$, which depend on the initial and final spins $J_i$, $J_f$, and on the mixing ratio $\delta$ of the transition:

$$A_{kk}(\gamma) = B_k A_k(\gamma).$$

For mixed transitions having multipolarities $L$ and $L'$ the standard expression for $A_k(\gamma)$ reads

$$A_k(\gamma) = \frac{[F_K(LLJ_fJ_i) + 2\delta F_K(LL'J_fJ_i) + \delta^2 F_K(L'L'J_fJ_i)]}{(1+\delta^2)}.$$

Here, the mixing ratio is in the convention of Krane and Steffen [19] and the $F_k$ are the usual $F$ coefficients. The value of $B_k(J)$ for maximum alignment, $B_k^\circ(J)$ are tabulated [18]. The attenuation coefficients

$$\alpha_k = B_k(J)/B_k^\circ(J)$$

relate the actual orientation parameters to the $B_k^\circ(J)$.

The spectra collected at the aforementioned angles were analyzed to extract information on level spins and $\delta[(L = 1)/(L' = 2)]$ mixing ratios.

A minimum $\chi^2$ procedures was applied for the analysis of the angular distribution data, with $A_{00}$, $A_{22}$, and $A_{44}$ as free parameters. The adopted $Q_k$ values were numerically evaluated following Ref. [19]. It proved convenient to perform the analysis separately for each run and to combine the results by considering the weighted average of the three sets of values for $A_{22}$ and $A_{44}$. In all considered cases the values extracted for $A_{44}$ were compatible with zero, within the errors. As a consequence, only the experimental $A_{22}$ values were utilized in the analysis.

Examples of the analysis performed to deduce the $A_{22}$ coefficients are reported in Fig. 5 for the 903.8 keV, $8_1^+ \rightarrow 6_1^+$ transition and for the 984.4 keV transition deexciting the 3251 keV level, of unknown spin, to the $4_1^+$ state. The $A_{22}$ value extracted for the 903.8 keV transition has been used to evaluate the attenuation coefficient for the $J = 8$ state (see text below).

The $A_{22}$ values obtained in the present work are reported in column 5 of Table III. In column 6 are given those deduced by Samudra *et al.* [6], who measured $\gamma$-ray angular distribution and polarization in $^{98}$Ru, populated in the same reaction and at the same beam energy as in the present work. In order to extract the $A_{22}$ distribution coefficients through a

TABLE III. Level and transition energies (except those of the 2670 keV level, identified in the present work) and spin-parities of the initial and final levels in columns 1–3 are from Ref. [1]. The $A_{22}$ values obtained in the present work are reported in column 5 together with those by Samudra *et al.* [6], given in column 6. The spins (column 7) of the initial levels and the $\delta(L = 1/L' = 2)$ mixing ratios of the deexciting transitions (column 8) have been deduced from the weighted averages of the $A_{22}$ coefficients of columns (5) and (6). The present $\delta$ values are compared with those (column 9) obtained by DuMarche' *et al.* [16] from angular distribution measurements. In some cases the data of columns 7 and 8 have been evaluated for a $J_i$ or $J_f$ spin (given in square parenthesis next to the data of interest) definitely assigned in other sections of the present work.

| $E_{\rm lev}$ (keV) | $J_i^\pi$ | $E_\gamma$ (keV) | $J_f^\pi$ | $A_{22}$ | $A_{22}$ [6] | $J_i$ | $\delta$ | $\delta$ [16] |
|---|---|---|---|---|---|---|---|---|
| 652.4 | $2_1^+$ | 652.4 | $0_1^+$ | 0.082(18) | 0.087(5) | | | |
| 1397.8 | $4_1^+$ | 745.4 | $2_1^+$ | 0.129(19) | 0.136(6) | | | |
| 1414.3 | $2_2^+$ | 761.8 | $2_1^+$ | 0.02(2) | 0.01(1) | | $-0.25^{+0.14}_{-0.05}$ or $+6.0^{+2.3}_{-2.7}$ | |
| | | 1414.3 | $0_1^+$ | 0.046(37) | 0.057(14) | | | |
| 1797.0 | $3_1^+$ | 382.7 | $2_2^+$ | −0.117(30) | −0.091(14) | | $+0.02^{+0.10}_{-0.16}$ or −3.5(12) | $(0.4^{+1.7}_{-0.3})$ |
| | | 398.8 | $4_1^+$ | 0.08(6) | 0.06(4) | | $-0.22^{+0.07}_{-0.16}$ or $-5.2^{+1.2}_{-1.7}$ | |
| 1817.2 | $(2)^+$ | 1164.8 | $2_1^+$ | −0.01(3) | −0.03(2) | 0–3 | | |
| 2012.7 | $3_2^+$ | 614.9 | $4_1^+$ | −0.111(36) | −0.108(11) | | $+0.24^{+0.20}_{-0.10}$ or $> 3$ | |
| 2222.5 | $6_1^+$ | 824.7 | $4_1^+$ | 0.184(18) | 0.187(5) | | | |
| 2266.5 | $4_2^+$ | 253.8 | $3_2^+$ | −0.365(54) | −0.360(20) | | −0.9 (0.5) | $(3.5^{+2.0}_{-1.2})$ |
| | | 469.5 | $3_1^+$ | 0.114(42) | 0.135(9) | | $+0.45^{+0.14}_{-0.08}$ or $+4.2^{+0.06}_{-0.13}$ | $(-0.8^{+0.3}_{-0.6})$ |
| | | 868.4 | $4_1^+$ | 0.04(4) | −0.07(2) | | $-0.37^{+0.32}_{-0.12}$ or $+2.1^{+1.0}_{-1.2}$ | |
| 2426.9 | $(2^+)$ | 610.0 | $(2)^+$ | −0.091(33) | −0.110(80) | 2,3 ($J_f = 2$) | $-1.5^{+0.8}_{-5.3}$ ($J_i = 2$) | |
| | | 629.8 | $3_1^+$ | | 0.17(7) | 2,3,4 | −0.04(45) ($J_i = 2$) | |
| 2547.0 | $(5,6)^+$ | 1149.2 | $4_1^+$ | 0.19(2) | 0.17(1) | 4,5,6 | 0.44(10) or $3.6^{+0.5}_{-1.0}$ ($J_i = 5$) | |
| 2656.5 | $(5^-)$ | 1258.7 | $4_1^+$ | −0.11(2) | −0.08(1) | 3,4,5 | | $> -0.1$ |
| 2659.6 | $(3^+,4)$ | 862.7 | $3_1^+$ | −0.074(43) | −0.064(16) | 2,3,4 | | |
| 2670.4 | | 1256.1 | $2_1^+$ | −0.01(4) | | 0-3 | | |
| 2720.0 | (3) | 1322.2 | $4_1^+$ | −0.09(5) | −0.05(4) | 3,4,5 | | |
| 2809.3 | $(2^+)$ | 542.8 | $4_2^+$ | | 0.18(4) | 3-6 | | |
| 2867.3 | $(6^+)$ | 320.3 | $(5,6)^+$ | 0.11(5) | 0.08(26) | 4–7 ($J_f = 5$) | | |
| 3064.8 | $(3^+)$ | 1667.0 | $4_1^+$ | −0.18(8) | −0.08(5) | 3,4,5 | | |
| 3126.3 | $8_1^+$ | 903.8 | $6_1^+$ | 0.232(27) | 0.230(20) | | | |
| 3190.2 | $(8^+)$ | 967.7 | $6_1^+$ | 0.192(22) | 0.210(30) | 5–8 | | |
| 3245.2 | $(6^+)$ | 978.8 | $4_2^+$ | 0.251(32) | 0.200(40) | 5,6 | | |
| 3250.6 | | 984.4 | $4_2^+$ | −0.111(34) | | 3,4,5 | | |
| 3283.3 | $(7)^-$ | 1060.6 | $6_1^+$ | −0.115(29) | −0.130(30) | 5,6,7 | | |
| 3538.5 | $(6^+,7,8^+)$ | 412.1 | $8_1^+$ | 0.197(80) | 0.190(90) | 6–9 | | |
| | | 991.8 | $(5,6)^+$ | 0.175(67) | | 6,7 ($J_f = 5$) | | |
| 3852.5 | | 569.0 | $(7)^-$ | 0.277(42) | | | | |
| 4000.6 | $10_1^+$ | 874.3 | $8_1^+$ | 0.286(65) | | | | |

minimum $\chi^2$ procedure to the angular distributions they kept $A_{44} = 0$.

Since our values of the $A_{22}$ coefficients are compatible with (in most cases very close to) those of Samudra *et al.* [6], we used, wherever possible, the weighted average of the two $A_{22}$ values to extract the information on spins and mixing ratios reported in columns 7 and 8 of Table II.

To overcome the problem related to the unknown alignments, we first considered the $A_{22}$ coefficients of the transitions reported in Table II which have pure $E2$ multipolarities. In this case the $\alpha_2$ values for the relevant levels can be directly extracted from the relation

$$\alpha_2 = A_{22}/B_2^\circ(J)Q_2A_2.$$

The values so obtained for the attenuation coefficients are reported in Fig. 6, as a function of the spins of the relevant states. It is seen that the $\alpha_2$ values lie approximately on a straight line and that the values, up to $J = 6$, are very well determined (errors are less than 1%).

We have then compared the experimental $A_{22}$ values for the other transitions to those calculated for any assumed $J$ and any possible $\delta$, in order to obtain information on spins and/or mixing ratios. We used for the attenuation coefficients the values extracted from the plot in Fig. 6, assigning to each $\alpha_2$ value a $J$-independent, conservative uncertainty of $\pm 0.05$.

An example of the analysis is given in Fig. 7, where the $A_{22}$ values, calculated in the hypothesis of $J_i = 5$ (spin assigned in the present work) for the 1149.2 keV transition which deexcites the 2547 keV level to the $4_1^+$ state, are compared to the experimental value. In this case, as in most of the cases investigated, two values of $\delta$ are possible.

The results of the analysis are reported in Table III. The deduced information on $J_i$ and on the mixing ratios are given in columns 7 and 8, respectively.

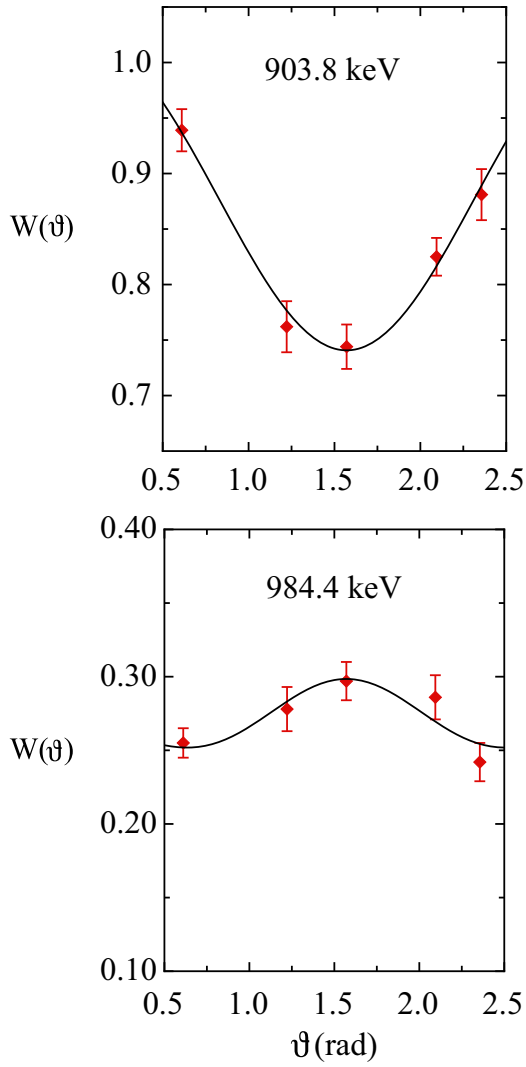


FIG. 5. Angular distribution of the 903.8 (upper panel) and 984.4 keV (lower panel) transitions deexciting the 3126 and 3251 keV levels, respectively. The continuous curve represents the function $W(\theta)$ evaluated with the fitted parameters. The reported values (on an arbitrary scale) correspond to the data collected in a single run.

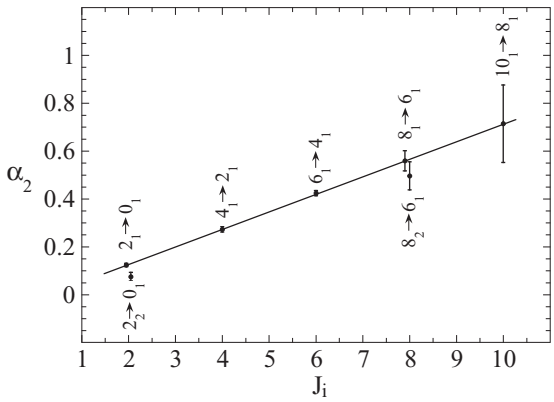


FIG. 6. Attenuation coefficient $\alpha_2$ as a function of $J_i$.

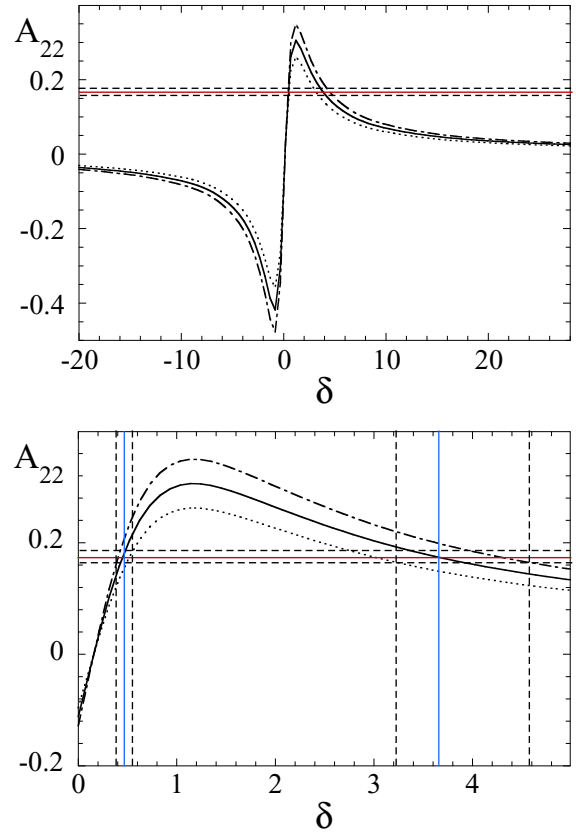


FIG. 7. Comparison of the experimental $A_{22}$ coefficient of the 1149.2 keV transition, deexciting the 2547 keV level to the $4_1^+$ state, with the values calculated for three values of the attenuation coefficient [$\alpha 2 = 0.30$ (dotted line), 0.35 (full line), and 0.40 (dashed line); see text for details], as a function of $\delta$, for $Ji = 5$. Upper panel: Extended range of $\delta$. Horizontal lines mark the experimental values (full line) and the associated uncertainties (dotted lines). Lower panel: Expanded view of the $\delta = 0$–5 region. Full vertical lines mark the deduced value of $\delta$, while dotted vertical lines mark the associated uncertainties.

### *3. γ-γ angular correlation analysis*

The data acquired in the $\gamma$-$\gamma$ coincidence measurements have also been utilized to extract information on spin values and mixing ratios $\delta$, for each considered $\gamma$ cascade. In order to avoid the need for accurate values of the absolute efficiencies of the different detectors, as a function of $\gamma$ energy, it proved convenient for any given $\gamma$-$\gamma$ cascade under study to normalize the raw coincidence data from each pair of germanium detectors to the corresponding ones from a reference cascade. In so doing, only relative efficiencies of any given counter are needed.

Since the statistics the $0_2^+ \rightarrow 2_1^+ \rightarrow 0_1^+$ cascade were rather poor, we chose to use as a reference the $4_1^+ \rightarrow 2_1^+ \rightarrow 0_1^+$ cascade, the most intense one. This, of course, has the disadvantage of introducing an additional unknown parameter, namely that which characterizes the alignment of the $J = 4_1^+$ state.

In the usual hypothesis of a Gaussian distribution of the population of the magnetic substates [18] the number of additional parameters for the upper level of any considered cascade can be reduced to one, namely to the standard

deviation $\sigma$. Clearly, there exists a one to one relation between $\sigma$ and each of the attenuation parameters $\alpha_2$ and $\alpha_4$ characterizing the angular distribution of the upper transition of the $\gamma$ cascade. The value of $\sigma$ for the reference cascade can thus be determined by exploiting the angular distribution data discussed in the previous section. In particular, for the $4_1^+ \rightarrow 2_1^+ \rightarrow 0_1^+$ cascade, we used the value of $\alpha_2$ [0.270(5)] given in Fig. 6.

The analysis of the angular correlation data was based on a dedicated computer code which utilizes the formulas given in Ref. [20]. To limit the number of additional parameters involved in a $J_1 \rightarrow J_2 \rightarrow J_3$ sequence, only cascades in which the lower $\gamma$ transition has a pure $E2$ multipolarity were considered.

The code computes, for each assumed value of the spin $J_1$, a table of $\chi^2$ values evaluated over a rectangular grid of equidistant values for $\sigma/J_1$ and arctan($\delta$) ($\delta$ being the mixing ratio of the $J_1 \rightarrow J_2$ transition to be investigated). The range of $\sigma/J_1$ has been restricted to an interval centered on the corresponding $\alpha_2$ value(s) of Fig. 6, of width $\pm 0.05$.

Essentially, the procedure compares the normalized coincidence data with those expected on the basis of the known angular correlation of the reference cascade and the postulated angular correlation specified (for the given geometry of the experimental setup) by $J_1$, $\sigma$, and $\delta$. In addition, for each $\sigma/J_1$-arctan($\delta$) pair, an overall normalization factor is computed analytically to provide the best $\chi^2$ value. In our case the number of degrees of freedom amounts to 17.

The entire procedure was repeated for all viable values of $J_1$ and the final choice of the spin value or range thereof was obtained by comparing the minimum values of $\chi^2$. In the case of definite spin assignment for $J_1$, the uncertainty (68% confidence level[1]) on $\delta$ was extracted in the standard way looking at the two-dimensional contour plot in the arctan($\delta$) and $\sigma/J_1$ space corresponding to an unitary increment of $\chi^2$ with respect to its minimum value.

Examples of the information on the spin of a given level obtained from angular correlation measurements are displayed in Fig. 8. The upper panel concerns the cascade originating from the 1817 keV level, the lower one that from the 2246 keV level. For the 1817 keV level the only possible spins are $J = 1,2$ because the transition connecting this state to the ground state has been definitely identified in the present work. In both cases spin $J = 2$ can be assigned to the levels.

The results obtained according to the procedure described above are summarized in Table IV.

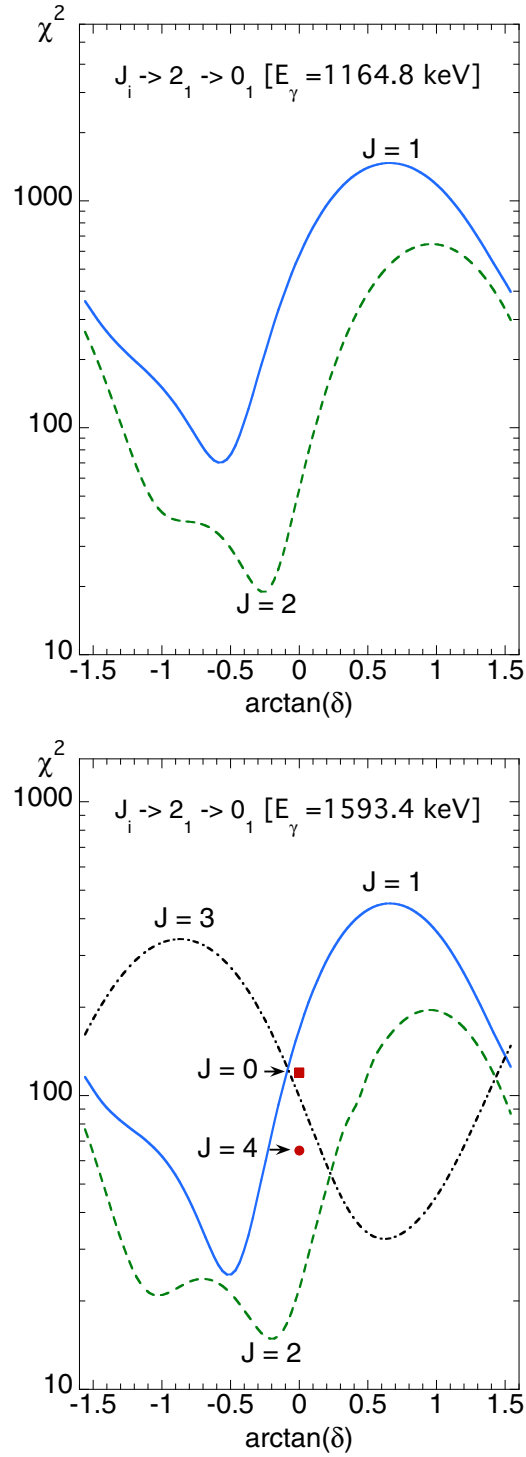


FIG. 8. Plot of $\chi^2$ versus arctan($\delta$) for the different hypotheses on the spin of the uppermost state of the reported cascades starting from the 1817 keV (upper panel) and 2246 keV (lower panel) levels, respectively.

## III. LEVEL SCHEME

The results obtained in the present work on the excitation energy pattern (up to about 4300 keV), $\gamma$ decay and spin-parity assignments, or limits thereof, of the $^{98}$Ru nucleus are summarized in Figs. 9–13. Levels and transitions energies as well as relative intensities of the transitions deexciting the single states are given in Table II.

Spins and parities reported in the figures are deduced from $\alpha_K$ conversion coefficients (Table I), angular distributions (Table III), angular correlations (Table IV) measurements, and

[1]As usual, this confidence level is referred to an estimate of the uncertainty on the single parameter $\delta$, independently of any statement about the uncertainty on $\sigma/J_1$.

TABLE IV. Information on spins deduced from angular correlation measurements for the levels reported in column 1 are given in column 5. The values deduced for the mixing ratios of the $\gamma$ transitions (column 3) are shown in column 6. Information previously available on the multipolarities of the transitions [1] is reported in the last column.

| $E_{\rm lev}$ (keV) | $J_1^\pi$ [1] | $E_\gamma$ (keV) | $J_2^\pi$ | $J$ | $\delta$ | $\delta$ [1] |
|---|---|---|---|---|---|---|
| 1414.3 | $2_2^+$ | 761.8 | $2_1^+$ | | $+11^{+8}_{-3}$ | $+13^{+4}_{-3}$ |
| 1817.2 | $(2)^+$ | 1164.8 | $2_1^+$ | 2 | $-0.27(6)$ | |
| 2012.7 | $3_2^+$ | 598.4 | $2_2^+$ | | $+0.14^{+0.06}_{-0.10}$ | +2.8(12) |
| | $3_2^+$ | 614.9 | $4_1^+$ | | $-0.35(5)$[a] | $M1+E2$ |
| 2245.8 | $(2^+,3^+)$ | 1593.4 | $2_1^+$ | 2 | $-0.19^{+0.10}_{-0.11}$ | |
| 2266.5 | $4^+$ | 868.4 | $4^+$ | | $2.3^{+1.5}_{-0.8}$ | $M1+E2$ |
| 2276.8 | $(2^+)$ | 879.2 | $4_1^+$ | 3,4 | | |
| | | 1624.2 | $2_1^+$ | 2,3, 4 | | |
| 2426.9 | $(2)^+$ | 1774.5 | $2_1^+$ | 2 | $0.42^{+0.07}_{-0.05}$ | |
| 2547.0 | $(5,6)^+$ | 1149.2 | $4_1^+$ | 5 | 0.37(5) | $M1,E2$ |
| 2656.5 | $(5^-)$ | 1258.7 | $4_1^+$ | 3,5 | | |
| 2720.0 | (3) | 1322.2 | $4_1^+$ | 3–6 | | |
| 2867.3 | $(6^+)$ | 644.8 | $6_1^+$ | 4,6,7,8 | | |
| 3016.8 | | 1619.0 | $4_1^+$ | 2–5 | | |
| 3064.8 | $(3^+)$ | 1667.0 | $4_1^+$ | 3–6 | | |
| 3069.2 | | 846.6 | $6_1^+$ | 5,6 | | |
| 3190.2 | $(8^+)$ | 967.7 | $6_1^+$ | 7,8 | | |
| 3283.3 | $(7)^-$ | 1060.6 | $6_1^+$ | 5,7 | | $E1$ |

[a]The sign of $\delta$ is at variance with the one of Table III.

from the information provided by the decay pattern (Table II). For spin-parity assignments the additional criteria adopted are the following:

(1) the triangular relations between $J_i$, $J_f$, and the multipolarity of the $\gamma$ ray must be respected;
(2) transitions between states differing by more than 2 spin units must be excluded;
(3) no pure $M2$ transition could be in competition with $E1,M1,E2$ transitions deexciting a given level.

We would like just to comment on a few cases where data of Ref. [1] are not supported by our findings.

(1) We do not observe a 567 keV transition reported by NDS as deexciting the 3853 keV, $9^-$ level to the 3283 keV state of spin $J=5,7$ (see Table IV). The presence of such a transition (together with the just mentioned restrictions on $J$) would imply a $J^\pi=7^-$ assignment to the latter. However, a negative parity would be incompatible with the decay of the 3283 keV state to the 2657 keV level, which, from angular correlation measurements (see Tab. IV) and from the identification of the 643.9 keV transition to the $3_2^+$ state, turns out to have $J^\pi=3,5^+$. The positive parity of the 3283 keV state is also confirmed by the $K$-conversion coefficient of the 1060.6 keV transition (see Table I) connecting this level to the $6_1^+$ state.
(2) Reference [1] suggests as possible spin-parities for the 3538 keV level $J^\pi=6^+,7,8^+$. At the same time it reports the existence of a 312 keV transition populating this level from the 3852 keV, $9^-$ state. This would exclude the spin $J=6$ and would imply negative parity for $J=7$. We do not observe a 312 keV transition and find $J^\pi=6^+,7^+$ as possible values for this level.
(3) The $J^\pi=7^-,8^+$ values suggested in NDS for the 3579 keV level were based on its population by a 272 keV transition from the $9^-$ state. The absence of such a transition and the present results give $J^\pi=5^+,6,7^+$ as possible values.

We would also remark on some differences with the data reported in Ref. [5]. On the basis of the results presented in Table II we can exclude that the states at 2246 and 2374 keV have $J^\pi=0^+$. It is considered by Cakirli *et al.* [5] as the most likely value because they do not observe any transition deexciting these states.

Regarding the 2276 keV level, it is not clear how the assignment or suggestion $J^\pi=2^+$ has been obtained. It is in disagreement with the possible $J^\pi=3^+,4^+$ values of the present work.

## IV. DISCUSSION

Theoretical investigations of the even isotopes of the ruthenium chain have made clear from the very beginning [21] that the nuclear structure changes from vibrational to $\gamma$ unstable in going from the $^{98}$Ru isotope to the heavier ones. However, a description of the $^{98}$Ru structure in terms of the pure vibrational model has proved to be inappropriate, which explains the great interest that has arisen about the intriguing features of the low excitation-energy pattern. Actually, the fact that this nucleus has a $4_1^+,2_2^+,0_2^+$ triplet at an energy ($\simeq$ 1.4 MeV) about twice that of the $2_1^+$ state and a multiplet, including the $6_1^+$ state, at an energy ($\simeq$ 2.2 MeV) about triple that of the $2_1^+$ state would suggest a vibrational structure.

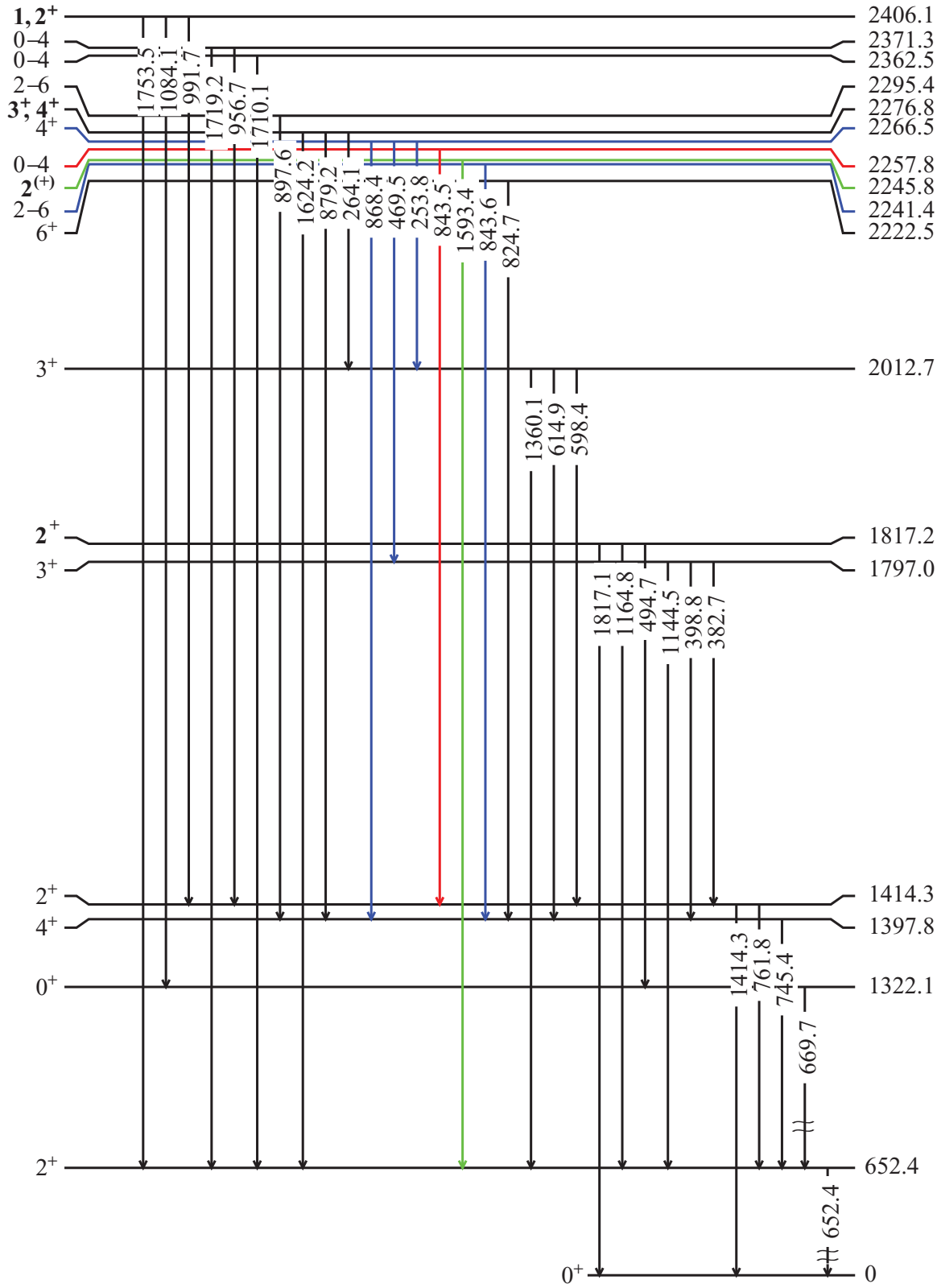


FIG. 9. Decay level scheme of $^{98}$Ru up to ∼2400 keV. Energies of levels and transitions are given in keV. New information on $J^+$ is reported in boldface characters.

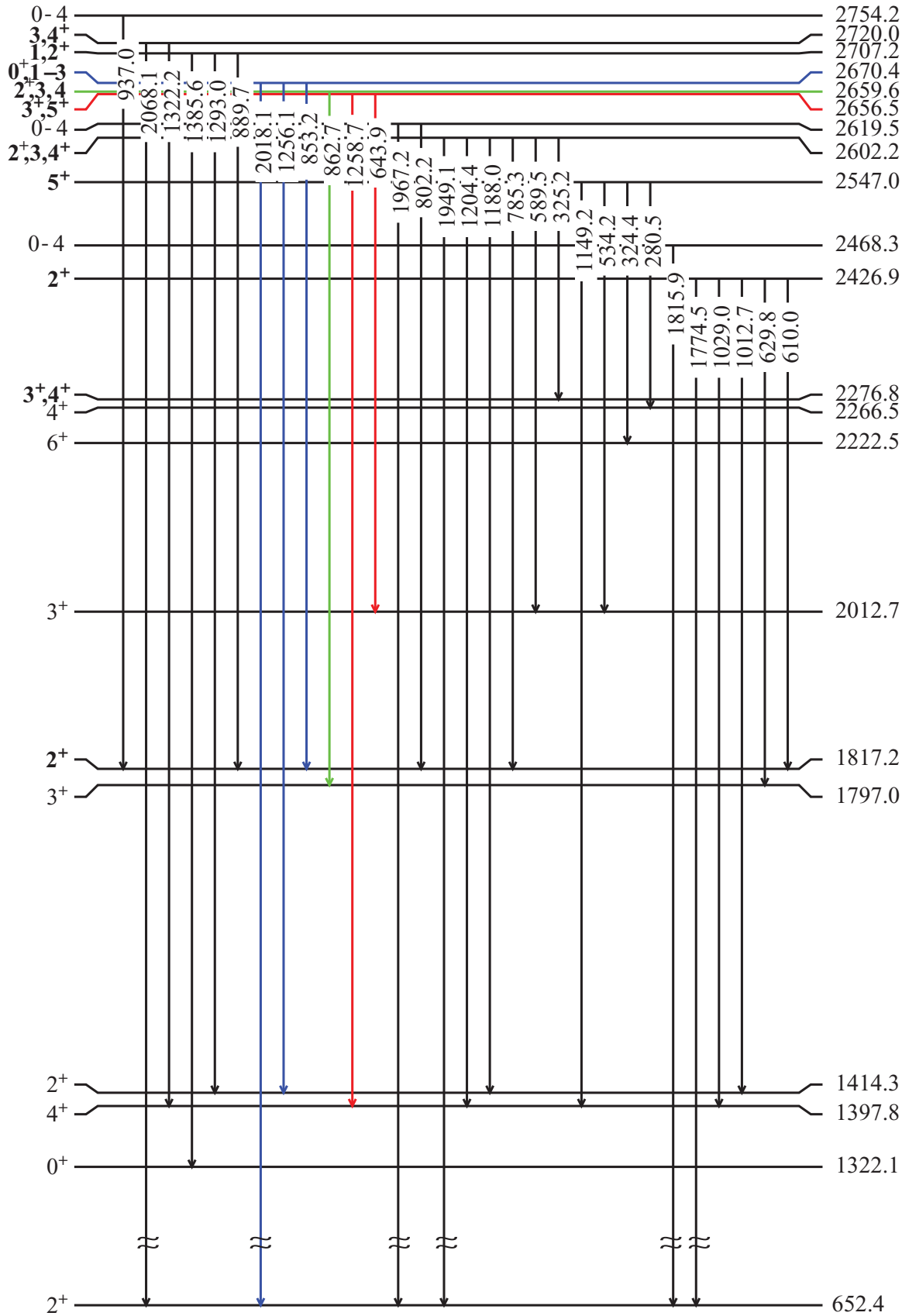


FIG. 10. Same as for Fig. 9 except for levels above 2400 keV.

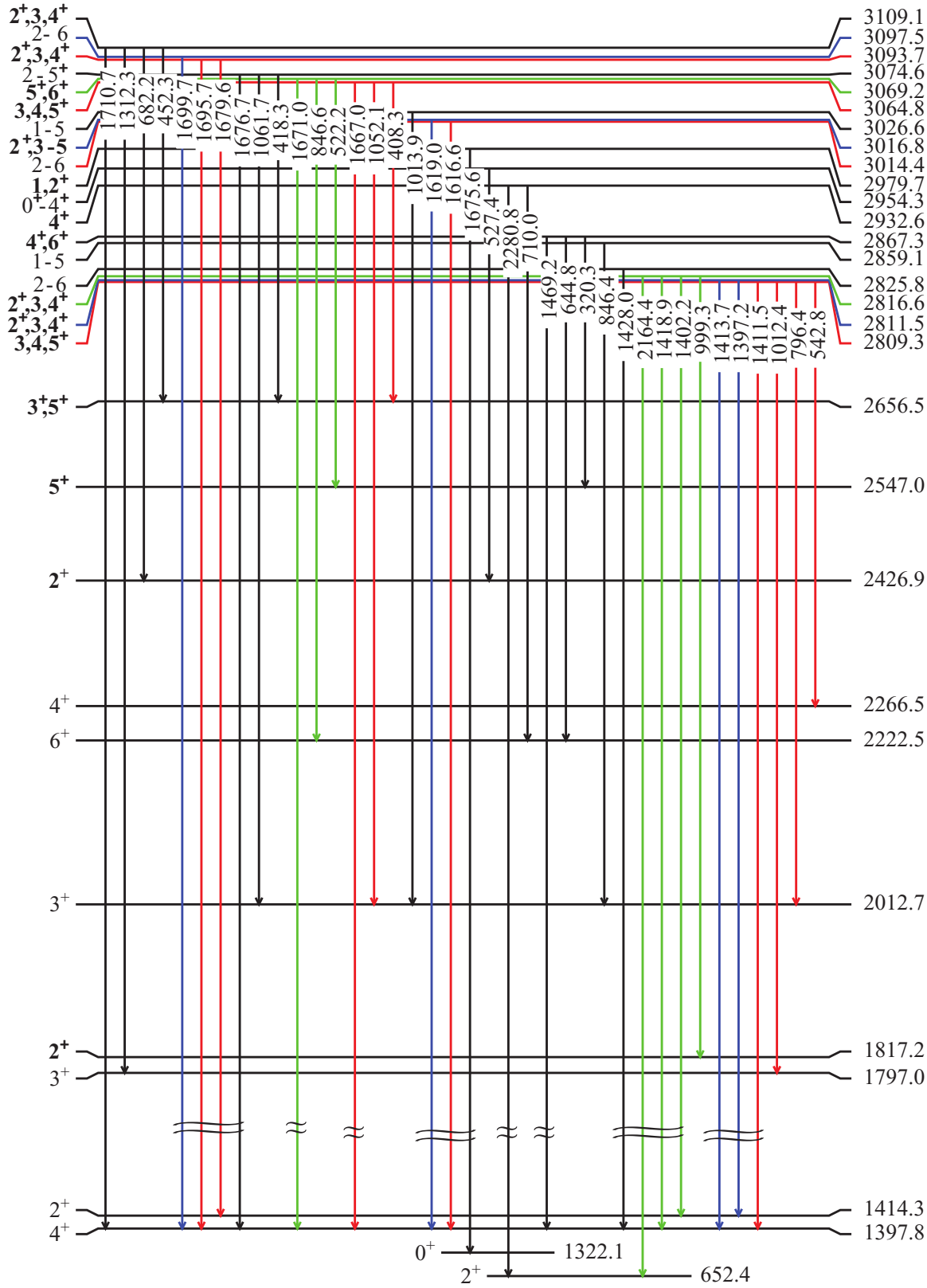


FIG. 11. Same as for Fig. 9 except for levels above 2800 keV.

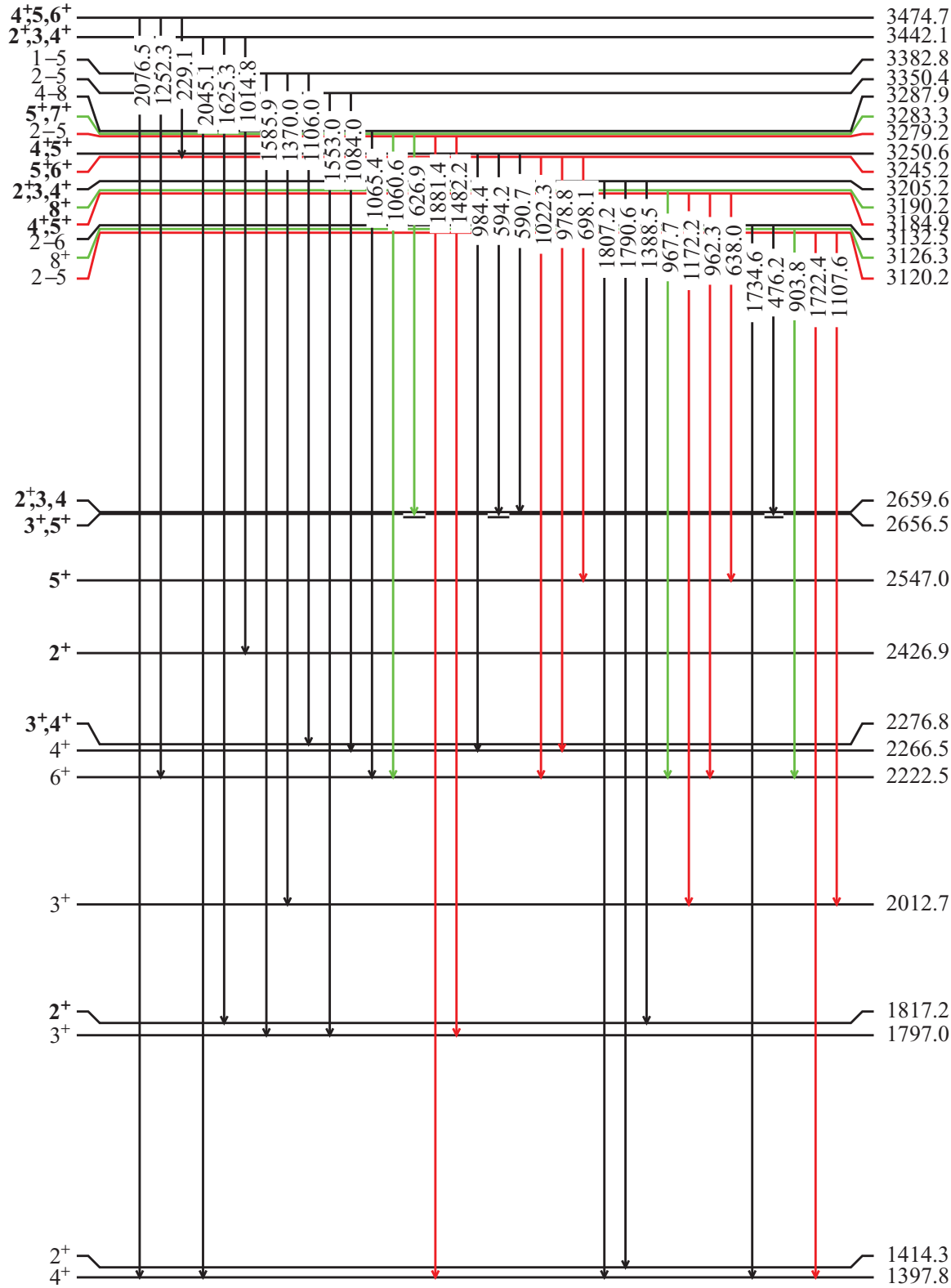


FIG. 12. Same as for Fig. 9 except for levels above 3100 keV.

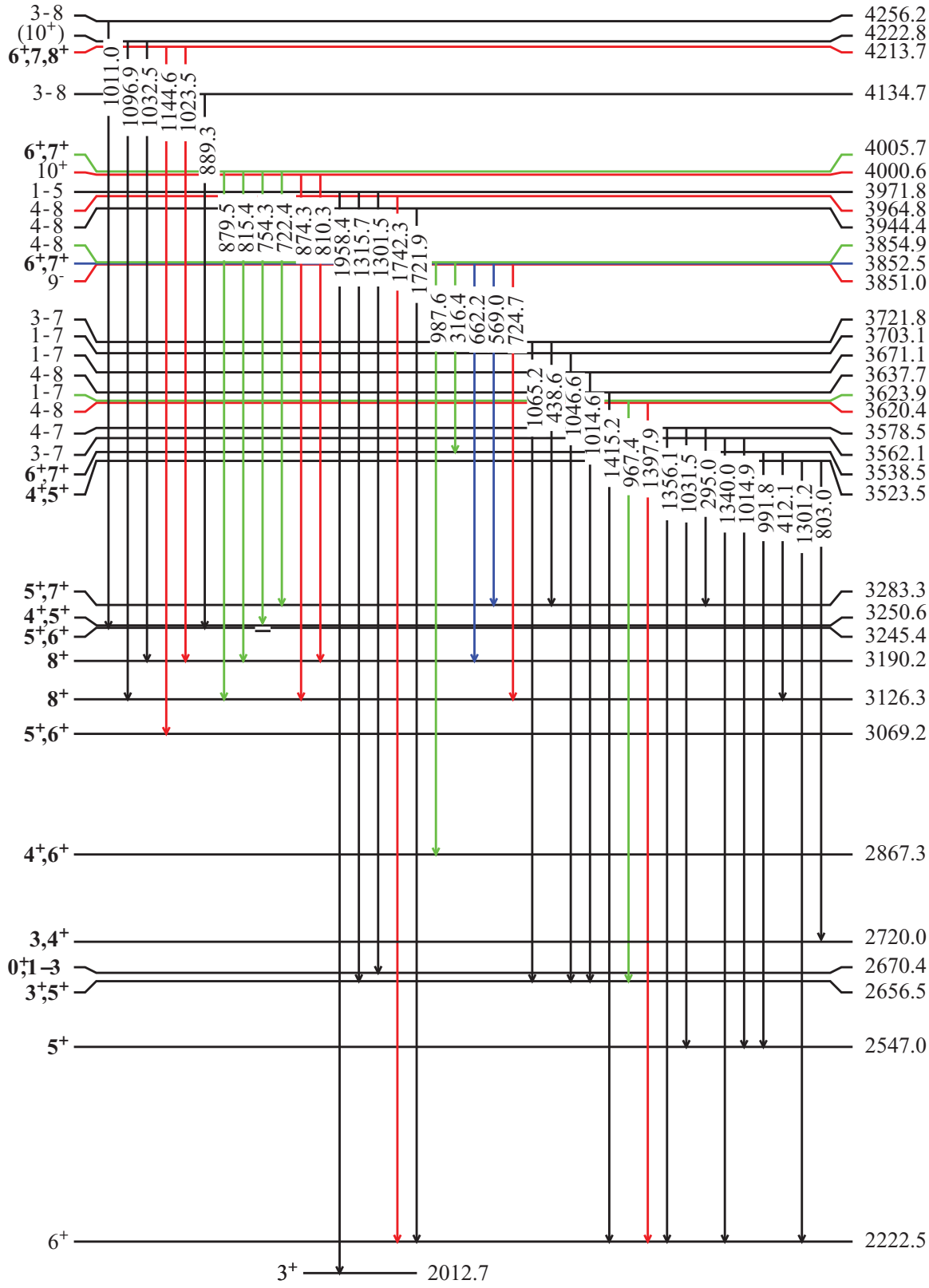


FIG. 13. Same as for Fig. 9 except for levels above 3500 keV.

However, the presence of two states at $\simeq$ 1.8 MeV, which do not fit such a scheme, as well as the decay properties of states belonging to the multiplet at $\simeq$ 2.2 MeV and the reduction of the $B(E2)$ transition strengths of the ground state band with increasing $J$ makes such an interpretation questionable.

Different models, such as the shell model [22] and the two quasiparticles coupled to a symmetric rotor model [6] have met limited success in describing the $^{98}$Ru structure.

A comparison with the U(5) limit of the IBA-1 model proved that the experimental excitation energies of the yrast states begin to significantly deviate from the calculated values beyond $J = 8$ [16]. Also a systematic search in different mass regions of nuclei presenting a vibrational character revealed that the U(5) limit is not appropriate to describe the $^{98}$Ru nucleus [23].

The difficulty of achieving a reasonable description of this nucleus became more and more apparent as the knowledge of the level structure increased. Cakirli *et al.* [5] have provided new experimental data on the decay pattern, which include a set of limits on the intensity of unobserved transitions. From comparison with the harmonic and anharmonic models, these authors conclude that "above the two-phonon levels there are no reasonable candidates for three phonon levels," so that in $^{98}$Ru there is "an almost complete breakdown of the vibrational structure."

The data acquired in the present work highlight that many transitions have large or predominant $M1$ components. This suggests that a model space larger than those of models like the anharmonic or the IBA-1 ones is necessary.

The IBA-2 model predicts [24–26] whole groups of states of mixed symmetry character, in addition to states fully symmetric (FS) in the proton-neutron degrees of freedom, which are the counterpart of the IBA-1 model states. They are characterized by a decay to FS states through $M1$ transitions, which are forbidden among FS states.

In the early 1980s Van Isacker and Puddu [27] used the IBA-2 model for a systematic study of the available spectroscopic data of the even Ru isotopes. All the states considered turned out to have FS character, apart from the $2^+_3$ state and, possibly, the $3^+_1$ state.

Subsequently, Giannatiempo *et al.* [10,11] investigated, in the same model, the structure evolution along the even Ru chain, paying particular attention to the identification of states having MS character. In particular, for the $^{98}$Ru isotope, these authors performed a detailed comparison of the calculations with all the spectroscopic data then available, concerning excitation energies, electric and magnetic dipole moments of the $2^+_1$ state, $B(E2)$ strengths, and branching ratios. They obtained an overall good agreement mainly due to the identification of states of MS character.

The large amount of new data available thanks to the present work makes it possible a stringent test of the prediction of the IBA-2 model for this isotope. This will be the subject of a forthcoming paper.

## V. CONCLUSIONS

Measurements of $K$-internal conversion coefficient, singles, $\gamma$ angular distribution, $\gamma$-$\gamma$ coincidence, and angular correlation have been performed in the nucleus $^{98}$Ru, populated via the $^{97}$Mo($^3$He$,2n$) reaction. The identification of new levels and transitions, joined to spin-parity assignments or limits thereof and mixing ratios determinations, has largely improved knowledge of the excitation energy pattern and removed discrepancies present in the literature.

The improved knowledge of the decay scheme shows that the doubts expressed by many authors, as well as the conclusions drawn by Cakirli *et al.* [5], about the impossibility of considering $^{98}$Ru as a nucleus having a pure vibrational structure, are correct.

From our previous IBA-2 analyses [10,11] it turns out that many levels of mixed symmetry character are expected in the $\simeq$1.5–4 MeV energy region. Their presence could possibly account to a large extent for the very complicated structure of this nucleus, in particular for the occurrence of many transitions having large $M1$ components.

## ACKNOWLEDGMENT

The authors are very grateful to A. Carcassi, A. Pecchioli, and M. Ottanelli for their essential technical assistance.

[1] B. Singh and Z. Hu, Nucl. Data Sheets **98**, 335 (2003).
[2] E. Williams *et al.*, Phys. Rev. C **74**, 024302 (2006).
[3] M. J. Taylor *et al.*, Phys. Rev. C **83**, 044315 (2011).
[4] D. Radeck *et al.*, Phys. Rev. C **85**, 014301 (2012).
[5] R. B. Cakirli *et al.*, Phys. Rev. C **70**, 044312 (2004).
[6] G. S. Samudra, K. D. Carnes, F. A. Rickey, P. C. Simms, and S. Zeghib, Phys. Rev. C **37**, 605 (1988).
[7] B. Kharraja *et al.*, Phys. Rev. C **57**, 83 (1998).
[8] J. Kotila, J. Suhonen, and D. S. Delion, Phys. Rev. C **68**, 054322 (2003).
[9] F. Iachello and A. Arima, *The Interacting Boson Model* (Cambridge University Press, Cambridge, UK, 1987).
[10] A. Giannatiempo, A. Nannini, P. Sona, and D. Cutoiu, Phys. Rev. C **52**, 2969 (1995).
[11] A. Giannatiempo, A. Nannini, and P. Sona, Phys. Rev. C **58**, 3335 (1998).
[12] A. Nannini, A. Perego, and P. Sona, EPJ Web Conf. **66**, 02071 (2014).
[13] T. Fazzini, A. Giannatiempo, and A. Perego, Nucl. Instrum. Methods **211**, 125 (1983); A. Nannini, Ph.D. thesis, University of Florence, 1992 (unpublished).
[14] J. H. Hamilton, in *The Electromagnetic Interaction in Nuclear Spectroscopy*, edited by W. D. Hamilton (North-Holland, Amsterdam, 1975), p. 451.
[15] BrIcc v2.3S, http://bricc.anu.edu.au/index.php.
[16] E. H. Du Marchie, Van Voorthuysen, M. J. A. De Voigt, N. Blasi, and J. F. W. Jansen, Nucl. Phys. A **355**, 93 (1981).
[17] N. Nica, Nucl. Data Sheets **111**, 525 (2010).
[18] T. Yamazaki, Nucl. Data A **3**, 1 (1967).

[19] K. S. Krane and R. M. Steffen, Phys. Rev. C **2**, 724 (1970).
[20] D. D. Watson and G. I. Harris, Nucl. Data A **3**, 25 (1967).
[21] J. Stachel, P. Van Isacker, and K. Heyde, Phys. Rev. C **25**, 650 (1982).
[22] B. Kharraja *et al.*, Phys. Rev. C **61**, 024301 (1999).
[23] J. Kern, P. E. Garret, J. Jolie, and H. Lehmann, Nucl. Phys. A **593**, 21 (1995).
[24] A. Arima, T. Otsuka, F. Iachello, and I. Talmi, Phys. Lett. B **66**, 205 (1977).
[25] T. Otsuka, A. Arima, F. Iachello, and I. Talmi, Phys. Lett. B **76**, 139 (1978).
[26] F. Iachello, Phys. Rev. Lett. **53**, 1427 (1984).
[27] P. Van Isacker and G. Puddu, Nucl. Phys. A **348**, 125 (1980).